

CENTRAL STELLAR MASS DEFICITS IN THE BULGES OF LOCAL LENTICULAR GALAXIES, AND THE CONNECTION WITH COMPACT $z \sim 1.5$ GALAXIES

BILILIGN T. DULLO¹, ALISTER W. GRAHAM¹

¹ Centre for Astrophysics and Supercomputing, Swinburne University of Technology, Hawthorn, Victoria 3122, Australia;
 Bdullo@astro.swin.edu.au

Draft version March 7, 2013

ABSTRACT

We have used the full radial extent of images from the *Hubble Space Telescope*’s Advanced Camera for Surveys and Wide Field Planetary Camera 2 to extract surface brightness profiles from a sample of six, local lenticular galaxy candidates. We have modelled these profiles using a core-Sérsic bulge *plus* an exponential disk model. Our lenticular disk galaxies with bulge magnitudes $M_V \lesssim -21.30$ mag have central stellar deficits, suggesting that these bulges may have formed from ‘dry’ merger events involving supermassive black holes while their surrounding disk was subsequently built up, perhaps via cold gas accretion scenarios. The central stellar mass deficits M_{def} are roughly 0.5 to 2 M_{BH} (black hole mass), rather than ~ 10 to 20 M_{BH} as claimed from some past studies, which is in accord with core-Sérsic model mass deficit measurements in elliptical galaxies. Furthermore, these bulges have Sérsic indices $n \sim 3$, half light radii $R_e < 2$ kpc and masses $> 10^{11} M_{\odot}$, and therefore appear to be descendants of the compact galaxies reported at $z \sim 1.5$ to 2. Past studies which have searched for these local counterparts by using single-component galaxy models to provide the $z \sim 0$ size comparisons have over-looked these dense, compact and massive bulges in today’s early-type disk galaxies. This evolutionary scenario not only accounts for what are today generally old bulges—which must be present in $z \sim 1.5$ images—residing in what are generally young disks, but it eliminates the uncomfortable suggestion of a factor of 3 to 5 growth in size for the compact, $z \sim 1.5$ galaxies that are known to possess infant disks.

Subject headings: galaxies: elliptical and lenticular, cD – galaxies: fundamental parameter – galaxies: nuclei – galaxies: photometry – galaxies: structure

1. INTRODUCTION

It is now widely believed that *all* massive elliptical galaxies, and massive bulges in disk galaxies, house a supermassive black hole (SMBH) at their center (Magorian et al. 1998; Richstone et al. 1998; Ferrarese & Ford 2005). In the standard cosmological formation paradigm of the universe, galaxies grow hierarchically, such that smaller systems merge to build larger ones (e.g., White & Rees 1978; Khochfar & Burkert 2001). As galaxies containing SMBHs collide, their black holes will migrate to the center of the merger remnant through dynamical friction, and form a bound binary. The subsequent hardening of the black hole binary, following the dissipation of orbital energy and angular momentum to the nearby stars, impacts on the central stellar distribution of the newly merged galaxy. The gravitational slingshot ejection of these stars (from the binary’s loss cone) via three-body interactions involving the binary is thought to be responsible for the physical origin of the partially depleted nuclear regions in luminous “core-Sérsic” galaxies which experienced ‘dry’, i.e. gas poor, merger events (Begelman et al. 1980; Ebisuzaki et al. 1991; Faber et al. 1997; Milosavljević & Merritt 2001; Merritt 2006; Sesana 2010; Gualandris & Merritt 2012).

Given the above scenario, the sizes and mass deficits of partially depleted cores are thought to reflect the amount of galactic merging and the ensuing extent of damage caused by binary SMBHs (after having eroded any preexisting nuclear star clusters: Bekki & Graham 2010). Accurate measurements of the central stellar mass deficits

in “core-Sérsic” galaxies can therefore provide useful constraints on models of galaxy formation and evolution. A key concept is that such core formation is by and large a cumulative process in which the ejected mass from SMBH binaries scales both with the final SMBH mass and the number of mergers (e.g., Milosavljević & Merritt 2001; Merritt 2006). Some recent studies have additionally postulated enhanced core depletions as a result of recursive core passages of recoiled SMBHs (Gualandris & Merritt 2008), or due to the actions of multiple SMBHs from merging galaxies (Kulkarni & Loeb 2011).

To date, several quantitative studies of the central stellar mass deficit have focused on elliptical galaxies (e.g., Graham 2004; Trujillo et al. 2004; Merritt 2006; Kormendy & Bender 2009; Dullo & Graham 2012). Violent, major dry merger events are commonly, or at least traditionally, thought to produce these elliptical galaxies (Toomre & Toomre 1972; Barnes & Herquist 1992; Kauffmann & Haehnelt 2000). Furthermore, as noted above, dry merger events involving supermassive black holes are also typically thought to be responsible for producing elliptical galaxies with partially depleted cores. Therefore, some ambiguity exists regarding the mechanisms for the formation of the lenticular (S0) disk galaxies having depleted cores.

In 1936 Hubble introduced lenticular galaxies into the tuning fork diagram (Jeans 1928; Hubble 1929); they were added as a hypothetical transition type between elliptical and spiral galaxies. Later observation of the populations of lenticular and spiral galaxies in clusters revealed the dominance of lenticular galaxies (spiral galax-

ies) in local (in distant) clusters (e.g., Dressler 1980; Dressler et al. 1997; Couch et al. 1998; Fasano et al. 2000; Desai et al. 2007; Poggianti et al. 2009; Sil’chenko et al. 2010). This suggested an evolutionary transformation of S0 galaxies from spiral galaxies, where mechanisms such as ram pressure stripping (Gunn & Gott 1972; Quilis et al. 2000), galaxy-galaxy harassment (Moore et al. 1996), strangulation (Larson et al. 1980; Bekki et al. 2002; Kawata & Mulchaey 2008) and gas starvation by AGN (van den bergh 2009) were forwarded to account for the removal of disk gas and the subsequent quenching of star formation, thereby passively fading the spiral galaxies and erasing their spiral arms. These formation scenarios, however, do not in themselves explain the central stellar depletions observed in some S0 galaxies.

The theoretical work of Steinmetz & Navarro (2002) has suggested that a galaxy’s morphology is a transient phenomenon. In this hierarchical picture, classic elliptical galaxies are built through major mergers (of disk galaxies) and may progressively regrow stellar disks, by gas accretion, which remain intact only until the next significant merger (see Okamoto & Nagashima 2001; Governato et al. 2009; Pichon et al. 2011; Sales et al. 2011; Conselice et al. 2012 for supporting arguments). The number of such cycles may however be low (i.e. 1) rather than several (3 to 5). Likewise, Arnold et al. (2011) and Forbes et al. (2011) recently pointed out that S0s might form through a two-phase inside-out assembly with the inner regions built early via a violent major merger, and “wet” minor mergers subsequently contributing to the outer parts.

This assembly scenario is consistent with the observed presence of partially depleted cores in luminous S0 galaxies. It also suggests that their bulges, most of which we know are old (e.g., MacArthur, González & Courteau 2009, and references therein), were already around at $z \approx 1.5$ to 2. Graham (2013, his Fig. 1) revealed that the compact galaxies at $z = 1.5$ to 2 have masses and structural properties consistent with those of the brighter bulges in local disk galaxies. Rather than being the precursors of elliptical galaxies prior to significant size evolution, Graham (2013) advocated that some of these compact high- z galaxies may therefore be associated with the bulges of modern disk galaxies. Furthermore, in this scenario in which compact *galaxies* evolve into disk galaxies with compact bulges, the (high velocity)-end of the galaxy ‘velocity dispersion function’ would not be expected to evolve from $z \sim 1.5$ to 0, just as observed (Bezanson, van Dokkum & Franx 2012).

Regarding the analysis of surface brightness profiles, Trujillo et al. (2004) avoided the inclusion of S0 galaxies in their sample of well-resolved local galaxies because it was felt that the introduction of an 8-parameter model (5 or 6 core-Sérsic parameters for the bulge plus 2 for the exponential disk) might be considered excessive at that time. Ferrarese et al. (2006) also avoided introducing two additional disk parameters in their modelling of well-resolved early-type galaxies in the Virgo cluster; however because their sample included disk galaxies, their core-Sérsic parameters do not correspond to the bulge component¹. Although Kormendy et al. (2009) did fit a Sérsic

bulge plus an exponential disk to their S0 galaxies, they marked the core region by eye rather than objectively fitting a core-Sérsic bulge plus exponential disk model. Depending on the sharpness of the (inner core)-to-(outer Sérsic) transition region, this practice may substantially over-estimate the formal ‘break radius’ — which is not to be confused with the inner or outer edge of the transition region.

Here we endeavor to provide the most accurate measurements to date of the centrally depleted stellar mass in lenticular disk galaxies. This is achieved by simultaneously fitting both a core-Sérsic model to the bulge *and* an exponential model to the disk.

This paper is organized as follows. Our initial sample of six suspected lenticular galaxies with depleted cores, plus the data reduction, and the light profile extraction technique are discussed in Section 2. In Dullo & Graham (2012) we did not have a sufficient radial extent of these six galaxies’ light profiles to include a disk component. Here we are able to test if this may have slightly biased some of our previous measurements of the bulge parameters. Section 3 introduces the analytical models used to describe the light profiles of “core-Sérsic” lenticular galaxies, and Section 4 details our fitting analysis while in Section 5 we describe the method for measuring the mass deficits of the core-Sérsic lenticular galaxies. Our interpretations of the central stellar mass deficits in the context of core-Sérsic lenticular galaxy formation scenarios are discussed in Section 6. In Section 6.1 we discuss the formation of core-Sérsic lenticular galaxies, and in Section 6.2 we compare the physical properties of their bulges with those of compact galaxies at $z = 1.5$ to 2. In Section 6.3 we discuss the role of galaxy environment. Section 7 summarizes our main conclusions. At the end of this paper are two appendices. The first provides notes on the six individual galaxies studied in this paper and the second provides a response to the criticism of Dullo & Graham (2012) by Lauer (2012) regarding the identification of partially depleted cores.

2. DATA AND PHOTOMETRY

2.1. Sample selection

We have targeted the six ‘core-Sérsic’ lenticular² galaxies from the sample of 39 relatively bright, nearby, early-type galaxies analysed by Dullo & Graham (2012). This initial sample of 39 galaxies came from Lauer et al. (2005) who had claimed that they all have partially depleted cores. Using the core-Sérsic model rather than the Nuker model, Dullo & Graham (2012) subsequently revealed that seven of them did not have partially depleted cores relative to the inward extrapolation of their outer Sérsic profiles (see also 9.2). The six, suspected lenticular galaxies with depleted cores are listed in Table 1.

2.2. Imaging data

High resolution *Hubble Space Telescope* (*HST*) optical images of these galaxies were retrieved from the public *HST* data archive. We only used images from

larger than that of the triaxial bulge component (e.g., Meert et al. 2012). Use of this larger ‘galaxy’ Sérsic index can result in an inflated measurement of the bulge’s central mass deficit.

² The initial morphological classification was taken from the Third Reference Catalog, RC3, de Vaucouleurs et al. (1991).

¹ The outer flattened disk of a lenticular galaxy, if not accounted for, can effectively result in a single ‘galaxy’ Sérsic index which is

broad-band filters. While the *HST* Advanced Camera for Survey (ACS; Ford et al. 1998) Wide Field Channel (WFC) F475W and F850LP images, from the Virgo Cluster Survey GO-9401 program (PI: P. Côté), are available for NGC 4382, for the remaining five galaxies (NGC 507, NGC 2300, NGC 3607, NGC 3706 and NGC 6849) we used the Wide Field Planetary Camera 2 (WFPC2; Holtzman et al. 1995) F555W images taken from the following programs: NGC 507, NGC 3706 and NGC 6849 from the GO-6587 program (PI: D. Richstone); NGC 2300 from the GO-6099 program (PI: S. Faber) and NGC 3607 from the GO-5999 program (PI: A. Phillips). For NGC 3607, we also used the near-infrared NICMOS/NIC2 F160W image observed in the GO-11219 program (PI: A. Capetti) to enable us to better avoid this galaxy’s inner dusty spiral structure. Global properties and observation details of all the sample galaxies are listed in Table 1.

The WFPC2 consists of 3 wide field cameras (WF2, WF3 and WF4) and a high resolution Planetary Camera (PC1); each has a CCD detector with 800×800 pixels. The three wide field cameras have a $0''.1$ per pixel spatial sampling. The smaller, high resolution planetary camera (PC1), where each galaxy’s center had been placed, has a plate scale of $0''.046$ and a square $36'' \times 36''$ field of view (FOV).

Having two CCDs cameras with 2048×4096 pixels, the ACS Wide Field Channel has a $0''.049$ pixel scale and covers a $202'' \times 202''$ rhomboidal area.

Combining the constituent CCDs of each camera, the light profiles from the WFPC2 and ACS observations probe a large range in radius, $R \gtrsim 80''$. For comparison, Lauer et al. (2005, and references therein) deconvolved all six sample galaxy images with the PSF and provided profiles out to a maximum of $10''$. The greater radial extent that we now have, from high quality CCD imaging, enables us to better sample and measure the disk light.

While our WFPC2/F555W (roughly Jonson-Cousins *V*-band) images match Lauer et al.’s. (2005) *V*-band images, for NGC 4382 the ACS/F475W (roughly SDSS *g*) and ACS/F850LP (roughly SDSS *z*) data are transformed to the *V*-band using

$$g - V = 0.98 (g - z) - 1.43, \quad (1)$$

which is acquired here from the least squares fit to the $(g - V)$ and $(g - z)$ data shown in Fig. 1, see also Sirianni et al. (2005) and Kormendy et al. (2009). The zero points in the Vega magnitude systems, which are adopted here to calibrate the WFPC2 (Holtzman et al. 1995) and ACS (Sirianni et al. 2005) profiles, were taken from the STScI web site³.

2.3. Data Reduction

The WFPC2, ACS and NICMOS images, retrieved from the Hubble Legacy Archive⁴ (HLA), were processed using the standard HLA reduction pipeline. The reduction steps include bias subtraction, geometric distortion

³ The ACS/WFC images used here are taken from observations before 2006.

⁴ <http://hla.stsci.edu>

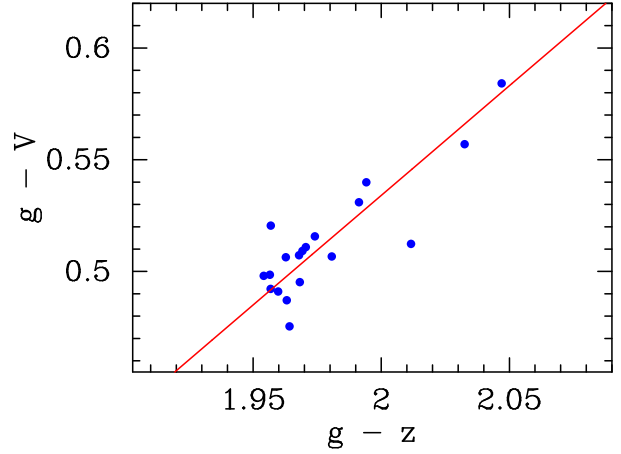


FIG. 1.— Photometric transformation from ACS *g* and *z*-band magnitude systems into WFPC2 *V*-band magnitude for NGC 4382. We use our *g* and *z*-band plus Lauer et al.’s (2005) *V*-band surface brightnesses of the galaxy at different radii to obtain the data points. The line is the least-squares fit to the data (Eqn. 1).

TABLE 1
GLOBAL PROPERTIES FOR OUR SAMPLE OF SIX SUSPECTED ‘CORE-SÉRSIC’
LENTICULAR GALAXIES.

Galaxy	Type	$M_{V,bulge}$ (mag)	D (Mpc)	σ (km s^{-1})	Filter	Exp. Time (s)
(1)	(2)	(3)	(4)	(5)	(6)	(7)
NGC 0507	S0	−22.56	63.7 ⁿ	306	F555W	1700
NGC 2300	S0	−21.33	25.7 ⁿ	261	F555W	1520
NGC 3607	S0	−21.55	22.2 ^t	224	F555W	160
					F160W	1151
NGC 3706	S0	−22.08	45.2 ⁿ	270	F555W	1400
NGC 4382	S0	−21.38	17.9 ^t	179	F475W	750
					F850LP	1210
NGC 6849	SB0	−22.51	80.5 ⁿ	209	F555W	900

Notes.—Col. (1) Galaxy name. Col. (2) Morphological type from RC3 (de Vaucouleurs et al. 1991). Col. (3) Absolute *V*-band bulge magnitude (galaxy magnitude for NGC 3706 since we (ultimately) adopt an elliptical morphology, see Section 4.1) obtained using our bulge-to-disk (B/D) flux ratios and absolute *V*-band *galaxy* magnitudes from Lauer et al. (2007b). These magnitudes are corrected for Galactic extinction, inclination and internal dust attenuation (Driver et al. 2008, their Table 1 and Eqs. 1 and 2) and $(1+z)^4$ surface brightness dimming, and adjusted using the distance from col. (4). Sources: (t) Tonry et al. (2001) after reducing their distance moduli by 0.06 mag (Blakeslee et al. 2002); (n) from NED (3K CMB). Col. (5) Central velocity dispersion from HyperLeda^a (Paturel et al. 2003).

^a(<http://leda.univ-lyon1.fr>)

correction, dark current subtraction and flat fielding using date-appropriate references: the WFPC2 (McMaster et al. 2008) and ACS (Pavlovsky et al. 2006) data and instrument handbooks provide detailed descriptions of these steps.

The automatic HLA reduction pipeline also subtracts the sky background values from the images. Contamination from a poor subtraction is a possibility which makes the automatic sky background estimation of the spatially extended galaxies slightly uncertain, it essentially affects the outermost parts (fainter regions) of such galaxies’ profiles. Having major-axis diameters of $\lesssim 4'$ and minor-axis diameters of $\lesssim 3'$ (using $\mu_B=25$ mag arcsec^{−2} as a reference level, NED), NGC 507, NGC 2300, NGC 3706 and NGC 6849 are within the WFPC2 field of view, thus, they are less prone to the sky subtraction errors. NGC 3607 and NGC 4382, however, extend beyond the

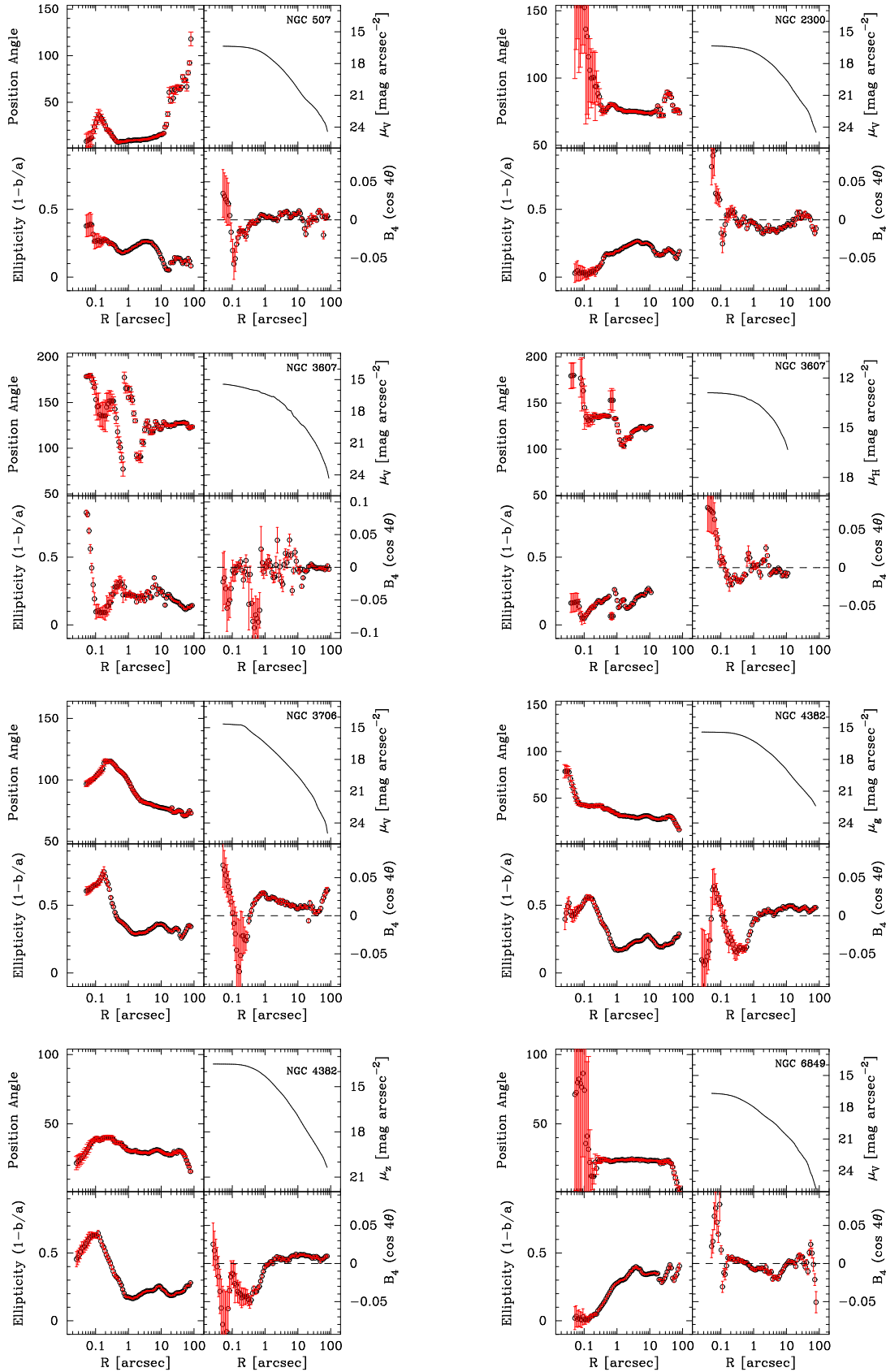


FIG. 2.— Major-axis surface brightness, ellipticity, position angle (measured in degrees from north to east) and isophote shape parameter (B_4) profiles for the galaxies in Table 1. Top right panels show the surface brightness profiles obtained with the F555W ($\sim V$ -band) filter, with the exception that a NICMOS NIC2 F160W (H -band) profile is also shown for NGC 3607, and NGC 4382 was imaged in the ACS F475W (g -band) and F850LP (z -band) filters.

WFPC2 and ACS field of views, respectively. Ferrarese et al. (2006) used a combination of the ACS and ground-based data to better constrain the sky level around NGC 4382, this data was later re-modelled by Dullo & Graham (2012, their Fig. 7). We find here that our light profile, and fit parameters for this galaxy, match those in Dullo & Graham (2012), indicating a small or zero sky subtraction error by the pipeline. This gives us some confidence that the outermost profile of NGC 3607 is also correct.

Finally, the images were masked to avoid the gaps between individual CCD detectors, the partially missing quadrant of the WFPC2 images, and regions including bright foreground stars, background galaxies, chip defects and galaxy dust lanes.

2.4. Surface photometry

The galaxy light profiles were extracted using the IRAF/STSDAS task ELLIPSE (Jedrzejewski 1987). We used the ELLIPSE task to construct the best-fitting concentric elliptical isophotes to the galaxy image starting from an initial elliptical isophote defined by the first guess values of the isophote center (X,Y), ellipticity (ϵ) and position angle (PA). We used median filtering, logarithmic spacing, and 3σ clipping for flagging deviant sample points at each isophote. To extract the major-axis light profiles, for all galaxies, the isophote centre (X,Y), ϵ and PA were set free to vary. For each galaxy we found that the isophote center was stable, i.e. within the small quoted error box.

The deviations of isophotes from perfect ellipses can be characterized well by higher order coefficients of the Fourier series expansion of the intensity (Jedrzejewski 1987). In particular, the coefficient of the $\cos 4\theta$ term, B_4 , is found to be of great importance in describing these deviations. Negative B_4 values imply that the isophotes are “boxy”, but, if B_4 is positive, the isophote will be identified as “disky”. Disky isophotes are frequently due to the presence of embedded disks in less massive, fast rotating, dissipative (gas rich) galaxies (e.g., Carter 1978, 1987; Davies et al. 1983; Bender et al. 1988; Peletier et al. 1990; Jaffe et al. 1994; Faber et al. 1997). In contrast, dissipationless violent relaxation of stars are often invoked to explain the boxy isophotes of triaxial, pressure-supported massive galaxies (Nieto & Bender 1989), which usually also contain hot X-ray emitting gas (e.g., Cattaneo et al. 2009).

In Fig. 2 we show the results of the ELLIPSE fitting. As noted in Rest et al. (2001), the isophotal parameters derived from the ELLIPSE fits tend to be more uncertain in the very inner regions ($R \lesssim 0.''3$); this feature is mainly due to the PSF and some contributions from the discrete sampling and subpixel interpolation of the IRAF fitting routine (Ravindranath et al. 2001). We note that while the disk/boxy isophotal deviations vary with radius in all of the six galaxies, NGC 507 and NGC 4382 have core regions which appear preferentially boxy within $1''$ (Fig. 2). Nieto & Bender (1989) reported that the S0 galaxy NGC 2300 has boxy inner ($1'' < R \lesssim 20''$) isophotes and disk/‘pointed’ outer ($20'' < R < 50''$) isophotes, in agreement with our result (Fig. 2).

In constructing ‘composite’ light profiles for each galaxy, we combine the very inner ($R \lesssim 1''$) Lauer et al. (2005) PSF-deconvolved, high resolution V-band light profile with our photometrically calibrated (V-band) pro-

file of the PSF-unaffected region beyond $\sim 1''$. For all the six galaxies in our sample, we find an excellent agreement (an overlap) between our light profiles and those published by Lauer et al. (2005) over the $1'' - 5''$ radial range.

3. MODELS FOR ‘CORE-SÉRSIC’ LENTICULAR GALAXIES

Given the two component (bulge/disk) nature of lenticular galaxies, we apply a bulge-to-disk photometric decomposition to the one-dimensional, major-axis surface brightness profiles of all the galaxies in our sample. When needed, a bar component is also included.

The radial intensity distribution of our lenticular galaxies’ disk component is modelled with an exponential function given by

$$I_{\text{disk}}(R) = I_{0d} \exp [-R/h], \quad (2)$$

where I_{0d} and h are the central intensity and scale length of the disk respectively.

We adopt the Ferrers (1877) function to describe the radial intensity distribution of the bar component, given by

$$I_{\text{bar}}(R) = I_{0\text{bar}} \left[1 - (R/a_{\text{bar}})^2 \right]^{n_{\text{bar}}+0.5}, \quad R < a_{\text{bar}},$$

$$I_{\text{bar}}(R) = 0, \quad R > a_{\text{bar}}, \quad (3)$$

where $I_{0\text{bar}}$, a_{bar} and n_{bar} are the central intensity, major-axis length and shape parameter of the bar, respectively (cf. Laurikainen et al. 2010).

Since the work by Caon et al. (1993) and Andredakis, Peletier & Balcells (1995), several studies revealed that, in general, the Sérsic (1963) model describes the underlying light distributions of both elliptical galaxies and the bulges of disk galaxies exceedingly well over a large radial range. This model can be written as

$$I(R) = I_0 \exp \left[-b_n \left(\frac{R}{R_e} \right)^{1/n} \right], \quad (4)$$

where $I_0 = I(R=0)$ is the central intensity. The quantity $b_n \approx 2n - 1/3$, for $1 \lesssim n \lesssim 10$ (e.g., Caon et al. 1993; Graham 2001) is a function of the Sérsic index n , and is defined in such a way to ensure that the half light radius, R_e , encloses half of the total luminosity. Reviewed in Graham & Driver (2005), the total luminosity of the Sérsic model within any radius R is given by

$$L_{T,\text{Ser}}(< R) = I_e R_e^2 2\pi n \frac{e^{b_n}}{(b_n)^{2n}} \gamma(2n, x), \quad (5)$$

where $\gamma(2n, x)$ is the incomplete gamma function and $x = b_n(R/R_e)^{1/n}$.

Systematic downward departures of the inner light profile relative to the inward extrapolation of the outer Sérsic model are known to exist in luminous galaxy/bulge light profiles. These are not exactly the same objects as “core” galaxies identified with the Nuker model (Lauer et al. 1995; Byun et al. 1996) or the double power-law model of Ferrarese et al. (1994). “Core-Sérsic” galaxies have partially-depleted cores relative to their outer Sérsic profile whereas “core” galaxies need not have any deficit but instead simply an inner power-law slope $\gamma < 0.3$. As detailed in Dullo & Graham (2012), the core-Sérsic

model (Graham et al. 2003), a combination of an inner power-law and an outer Sérsic function, provides a good representation of the brightness profiles of bulges in disk galaxies with depleted cores. The model is defined as

$$I(R) = I' \left[1 + \left(\frac{R_b}{R} \right)^\alpha \right]^{\gamma/\alpha} \exp \left[-b_n \left(\frac{R^\alpha + R_b^\alpha}{R_e^\alpha} \right)^{1/(\alpha n)} \right], \quad (6)$$

with

$$I' = I_b 2^{-\gamma/\alpha} \exp \left[b_n (2^{1/\alpha} R_b / R_e)^{1/n} \right]. \quad (7)$$

The term I_b denotes the intensity at the core's break radius R_b , γ is the slope of the inner power law, and α controls the sharpness of the transition between the inner power-law and the outer Sérsic profile. Both R_e and b_n have the same general meaning as in the Sérsic model.

4. FITTING ANALYSIS

Fig. 3 displays the best model fits to the major-axis surface brightness profiles of the 6 galaxies listed in Table 1. We follow the iterative fitting technique of Dullo & Graham (2012), minimizing the root mean square (rms) residuals to determine the best fit parameters that match the data. It is important to note that these profiles now cover a large range in radius (out to $R \gtrsim 80''$), giving both the core-Sérsic and the exponential models enough radial expanse to both quantify the curvature in the bulge profile (i.e. the Sérsic index) and define the disk scale length. Table 2 lists the fit parameters obtained from the adopted core-Sérsic plus exponential bulge+disk models.

Apparent from Fig. 3 is that the global light distribution of all the sample galaxies, except for NGC 3706 (E not S0) and NGC 6849 (barred), can be accurately represented by the core-Sérsic+exponential model with a small rms residuals $\lesssim 0.05$ mag arcsec $^{-2}$. If a single core-Sérsic model is fit to the light profile of a disk galaxy (i.e. a two-component system comprised of a flattened disk and a triaxial bulge), this would result in parameters that do not describe the triaxial bulge component of the galaxy, effecting in particular the Sérsic index, and ultimately the mass deficit measurement as happened in Ferrarese et al. (2006, See also Meert et al. 2012). Although NGC 3706 is classified as a lenticular galaxy in the RC3, we find that its light profile is best fitted by a single core-Sérsic model, without an exponential disk component. This suggests that the galaxy may be an elliptical galaxy misclassified as an S0 in the RC3, consistent with the conclusion of Laurikainen et al. (2010). As for NGC 6849, the 3-component bulge-bar-disk light profile is well described by the core-Sérsic bulge+Ferrers bar+exponential disk decomposition model (see Fig. 3 and Section 9.1.6).

While the V -band surface brightness profile of NGC 3607 is well described by the core-Sérsic bulge+exponential disk model, the $1''.31$ core radius of this fit is suspiciously larger than the $0''.22$ core radius reported by Richings et al. (2011) from their H -band profile analysis. The explanation is that a dusty nuclear spiral has caused a reduction to the inner V -band light profile. Our analysis of the PSF-affected H -band light profile (Fig. 3) gives a core radius of $0''.11$, which is in

fair agreement with the result found by Richings et al. (2011) but does not support a large core in this galaxy. Given that the core size we find with the PSF-affected H -band data is comparable to the seeing, coupled with the dusty spiral structure, we are unable to conclude if there is indeed any partially-depleted core in this galaxy, and as such we exclude it from our final analysis.

We have found that the bulge model parameters (Table 2) generally agree well with those from Dullo & Graham (2012). For NGC 2300, the contribution of the disk light to the inner $15''$ profile which we modelled in Dullo & Graham (2012) did however result in a break radius $R_b = 0''.98$ which is slightly larger than the one from this work ($R_b = 0''.53$). With the exception of this galaxy, the agreement between the break radii from these two studies is good, constrained to less than a 20% discrepancy. For each galaxy, we find that the V -band surface brightness at the break radius ($\mu_{b,V}$) given in Table 2 agrees with those presented in Dullo & Graham (2012) to within the range of error bar: there is $\sim 5\%$ discrepancy, which is well within the Dullo & Graham (2012) $\sim 10\%$ uncertainty range. We have also compared the inner power-law slopes (γ) from the two studies. We find that the new γ values (Table 2) are consistent with those reported in Dullo & Graham (2012).

The five core-Sérsic lenticular galaxies (Table 2) have bulge Sérsic indices $n \sim 3$, while typically for core-Sérsic elliptical galaxies n is greater than 3. This may be because, for a given magnitude, the bulges of disk galaxies appear to have lower Sérsic indices than elliptical galaxies of the same magnitude (Graham 2001, his Fig. 14). It may also be that the elliptical core-Sérsic galaxies from Dullo & Graham (2012) are brighter.

5. CENTRAL STELLAR MASS DEFICIT

The central stellar mass deficit (M_{def}) of ‘core-Sérsic’ galaxies is predicted to be generated mainly via the three-body encounters of the core stars with the inspiraling black holes in a merger remnant (e.g., Ebisuzaki et al. 1991; Milosavljević & Merritt 2001; Merritt 2006). Graham (2004) measured this stellar mass deficit from the luminosity difference L_{def} between the inward extrapolation of the outer Sérsic model and the (sharp-transition⁵) core-Sérsic model. This approach was adopted in subsequent works by Ferrarese et al. (2006), Merritt (2006) and Hyde et al. (2008). We adopt a slightly different methodology to those studies by using a finite value for α in Eq. 6 and thus a smoother transition region between the inner power-law and the outer Sérsic profile of the core-Sérsic model. The total core-Sérsic model luminosity (Trujillo et al. 2004; their Eq. A19) is given by

$$L_{T,CS} = 2\pi I' n (R_e/b^n)^2 \int_{b(R_b/R_e)^{1/n}}^{+\infty} e^{-x} x^{n(\gamma+\alpha)-1} \times [x^{n\alpha} - (b^n R_b/R_e)^\alpha]^{(2-\gamma-\alpha)/\alpha} dx, \quad (8)$$

where all the parameters have the same meaning as in Eq. 6. The difference in luminosity between the outer

⁵ Trujillo et al. (2004) set the transition parameter $\alpha \rightarrow \infty$ to obtain the 5-parameter sharp-transition core-Sérsic function given by their Eqn. 5.

TABLE 2
STRUCTURAL PARAMETERS.

Galaxy	Type	$\mu_{b,V}$	R_b (arcsec)	R_b (pc)	γ	α	n	R_e (arcsec)	R_e kpc	$\mu_{0d,V}$	h (arcsec)	$(B/T)_{Obs}$	$(B/T)_{Cor}$	i ($^\circ$)
(1)	(2)	(3)	(4)	(5)	(6)	(7)	(8)	(9)	(10)	(11)	(12)	(13)	(14)	(15)
NGC 0507	S0	16.38	0.33	102	0.07	5	2.19	5.34	1.65	21.03	27.69	0.32	0.43	0
NGC 2300	S0	16.61	0.53	70	0.08	2	2.20	7.69	1.02	20.39	21.08	0.42	0.57	44
NGC 3607	S0	—	—	—	—	—	2.39	7.75	0.84	19.16	18.61	0.40	0.57	59
NGC 3706 [†]	E	14.16	0.11	24	-0.02	10	6.36	42.08	9.18	—	—	—	—	53
NGC 4382	S0	15.01	0.27	24	0.07	5	2.65	11.14	0.99	19.50	35.07	0.28	0.40	39
NGC 6849 [‡]	SB0	16.67	0.18	69	0.20	5	3.23	7.77	2.98	20.72	16.93	0.31	0.46	55

Notes.—Structural parameters from fits to the V-band major-axis surface brightness profiles (Fig. 3). Col. (1) Galaxy name. Col. (2) Our adopted morphological classification. Col. (3)-(10) Best-fit bulge structural parameters from the core-Sérsic model, Eq. 6. Col. (11)-(12) Best-fit disk structural parameters from the exponential model, Eq. 3. Break surface brightness $\mu_{b,V}$ and disk central surface brightness $\mu_{0d,V}$ are in mag arcsec⁻². Col. (13) Expected V-band bulge-to-total (B/T)_{Obs} flux ratios obtained using Graham & Driver (2005, their Eq. 19). These ratios are corrected for Galactic extinction, surface brightness dimming, internal dust attenuation and inclination (Driver et al. 2008, their Table 1 and Eqs. 1 and 2) and listed in Col. (14). Col. (15) Disk inclination angles (i) are derived using the galaxies' major- and minor-axis diameters from NED. [†] We classify NGC 3706 as an elliptical galaxy based on our light profile analysis. [‡] The fit parameters for the bar component: $\mu_{0bar,V}=21.63$ mag arcsec⁻², $a_{bar}=29''.04$, and $n_{bar}=6.37$.

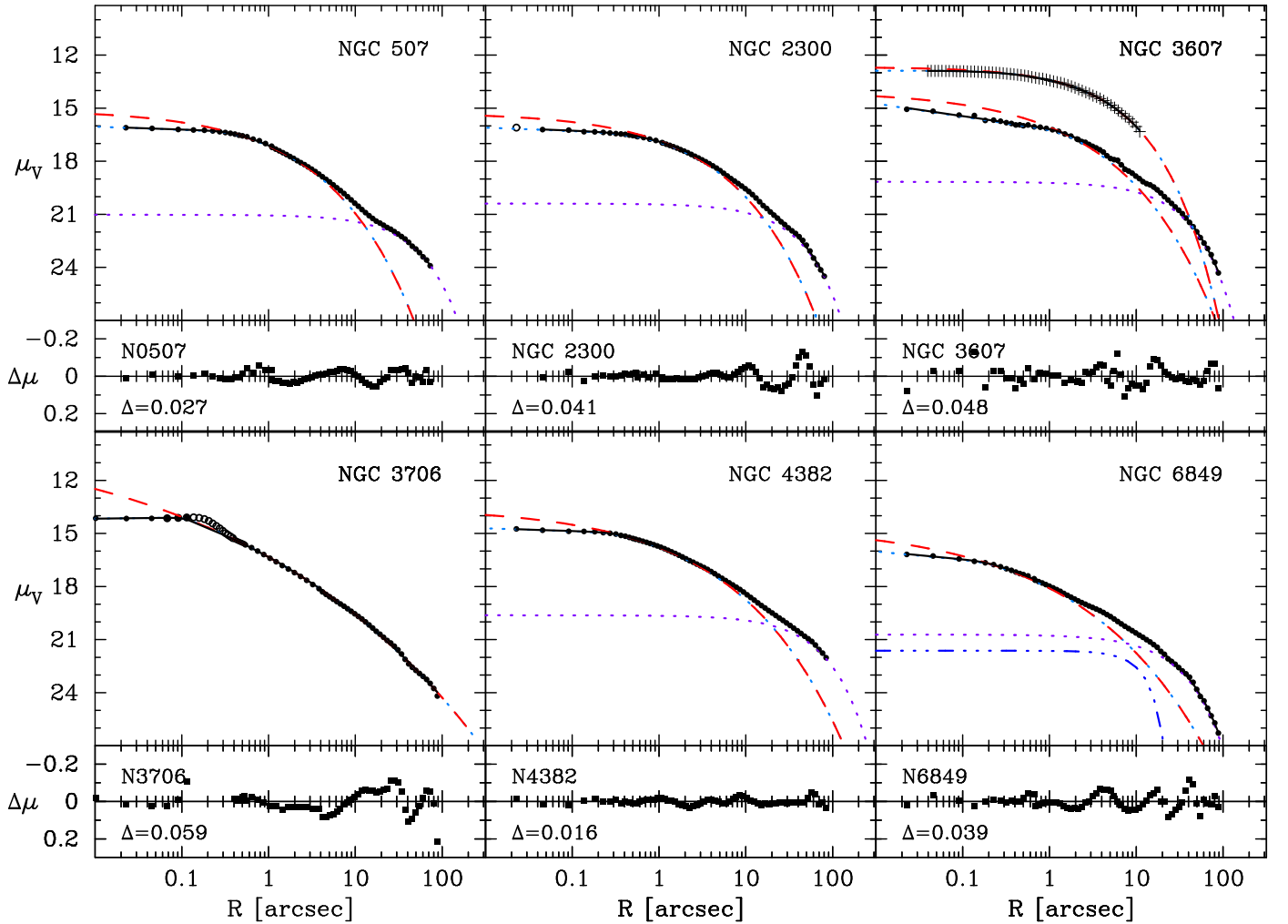


FIG. 3.— Fits to the major-axis surface brightness profiles of the galaxies in Table 1. For NGC 3607 (with a dusty nuclear spiral), the core-Sérsic model fit to the PSF-affected H -band data (crosses) is shown in addition to the core-Sérsic+exponential fit to the V -band data (dots). The dashed curves show the Sérsic component of the core-Sérsic fits to the data, while the dotted curves show the exponential function simultaneously fit to the large scale disks. The dash-dot-dot-dot curve shows the Ferrers function fit to the bar component of NGC 3607. The solid curves show the complete fit to the profiles, with the rms residuals, Δ , about each fit given in the lower panels. For NGC 3607, we only show the rms residual from the V -band profile fit, while Δ from its H -band profile fit is 0.014 mag arcsec⁻². Data points excluded from the fits are shown by the open circles (see Section 9).

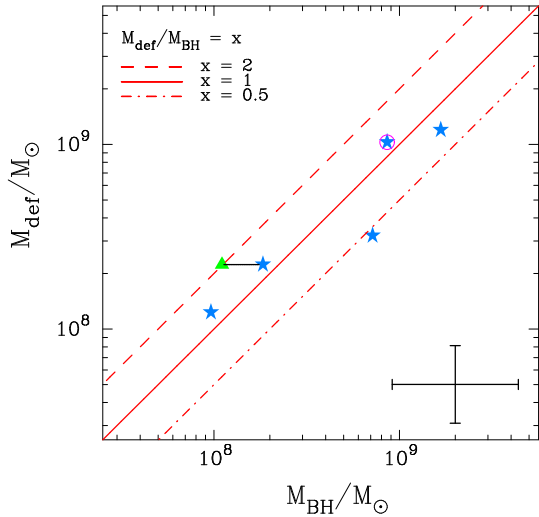


FIG. 4.— Central mass deficit (M_{def}) versus black hole mass (M_{BH}) for ‘core-Sérsic’ galaxies listed in Table 2 and 3. The only elliptical galaxy is circled. The M - σ relation presented in Graham et al. (2011) was used for estimating the SMBH masses of the galaxies. A horizontal solid line connects the two predicted black hole masses of NGC 6849: i) assuming it is a barred galaxy (triangle) and ii) considering it as a non-barred galaxy (star). A representative error bar is shown at the bottom of the panel.

Sérsic model (Eq. 5) and the core-Sérsic model (Eq. 8) is of course the central stellar flux deficit.

To convert the luminosity deficits into mass deficits, individual stellar mass-to-light (M/L) ratios were derived for each galaxy. To determine these ratios, we have made use of the available (preferentially nuclear) colours of the galaxies as well as the colour-age-metallicity- (M/L) diagram from Graham & Spitler (2009; their Fig A1). As in Graham (2004), we have assumed that the inner regions of these galaxies have an evolved (old) single population of stars.

For NGC 2300, NGC 3607 and NGC 4382, the nuclear $V-I$ colours of 1.33, 1.36 and 1.11, taken from Lauer et al. (2005), correspond to stellar M/L_V ratios of 5.0, 5.7 and 2.6, respectively. Using the HyperLeda database, NGC 507 and NGC 3706 have $V-I$ colours of 1.40 and 1.34, respectively, while NGC 6849 has $V-I=1.03$. From this, we obtain M/L_V ratios of 5.5, 5.2, and 2.4 for NGC 507, NGC 3706 and NGC 6849, respectively (see Table 3). These mass-to-light ratios were used to convert the stellar flux deficits into stellar mass deficits. These have been plotted in Fig. 4 against each galaxy’s expected black hole mass as derived from the $M-\sigma$ relation (Graham et al. 2011; the lower half of their Table 2) based on the σ values in Table 1.

As noted above, high-accuracy N-body simulations by Merritt (2006) revealed that the effect of multiple dissipationless mergers on core formation is cumulative, thus, the extent of core evacuation could reflect the amount of merging. He found that the total mass deficit after N ‘dry’ major mergers is $\approx 0.5NM_{\text{BH}}$, where M_{BH} is the final black hole mass. This result hinges on a key assumption that the central black hole would tidally disrupt infalling high-density satellites, thereby protecting any preexisting core (Faber et al. 1997; Boylan-Kolchin & Ma 2007).

Fig. 4 shows that the mass deficits for the ‘core-Sérsic’ lenticular galaxies (plus one elliptical galaxy) listed in

Table 2 are $M_{\text{def}} \sim 0.5 - 2M_{\text{BH}}$, which translates to a few (1 to 4) ‘dry’ major merger events. For reference, measurements of close galaxy pairs in real data (i.e. not simulations) suggest that massive galaxies ($> 10^{10.5}M_{\odot}$) have experienced 0.5 to 2 major mergers since $z \sim 0.7$ to 1 (e.g., Bell et al. 2004, 2006; Bluck et al. 2012; Man et al. 2012; Xu et al. 2012). Our figure is double this value, but it has no upper redshift constraint associated with it. The mean elliptical galaxy $M_{\text{def}}/M_{\text{BH}}$ mass ratio from Graham (2004) is 2.1 ± 1.1 , while the mean ratio from Ferrarese et al. (2006) is 2.4 ± 0.8 after excluding the S0 galaxy NGC 4382 from their sample (as they did at the end of their Section 5.2). We used the $M_{\text{BH}}-\sigma$ relation presented in Graham et al. (2011; the lower half of their Table 2) for estimating the SMBH masses of the five core-Sérsic galaxies shown in Table 3. While this $M_{\text{BH}}-\sigma$ relation was constructed by combining core-Sérsic and Sérsic galaxies, Graham & Scott (2012, their Table 3) have recently shown that core-Sérsic and Sérsic galaxies follow similar $M_{\text{BH}}-\sigma$ relations. They additionally reported an $M_{\text{BH}}-\sigma$ relation for their combined (core-Sérsic + Sérsic) galaxies which is consistent with the relation found by Graham et al. (2011). We find that, for all our core-Sérsic galaxies, the SMBH masses predicted using the Graham & Scott (2012) $M_{\text{BH}}-\sigma$ relations which are defined by the core-Sérsic, Sérsic or core-Sérsic + Sérsic galaxies agree with those used in this study (Table 3) within the range of error bars. We make use of Eq. 4 from Graham et al. (2011) and the σ -values in Table 1 and assume a 10% uncertainty on σ to estimate the 1σ uncertainty on each galaxy’s SMBH mass (Table 3).

For NGC 4382, Kormendy & Bender (2009) reported a mass deficit of $M_{\text{def}} \sim 1.3 \times 10^9 M_{\odot} \approx 13M_{\text{BH}}$ when using $M_{\text{BH}} = 1 \times 10^8 M_{\odot}$, while Gültekin et al. (2011) used Nuker model parameters and found a mass deficit of $M_{\text{def}} \sim 5.9 \times 10^8 M_{\odot} \approx 45.6M_{\text{BH}}$ when they assumed a very small black hole mass of $1.3 \times 10^7 M_{\odot}$. Ferrarese et al. (2006, see their Fig. 20) noted that the large-scale stellar disk of NGC 4382, which was incorporated into their single Sérsic fit to this galaxy, might have biased their $\sim 10M_{\text{BH}}$ mass deficit measurement. Indeed, their *galaxy* Sérsic index was $\approx 6-7$, while we have found that the bulge Sérsic index is less than 3. Our analysis of this bulge’s central stellar mass deficit yields $M_{\text{def}} \sim 1.2 \times 10^8 M_{\odot} \approx 1.3M_{\text{BH}}$ (using $M_{\text{BH}} = 9.55 \times 10^7 M_{\odot}$), smaller than the results of Ferrarese et al. (2006), Kormendy et al. (2009) and Gültekin et al. (2011).

Previously, Milosavljević & Merritt (2001), Milosavljević et al. (2002), Ravindranath et al. (2002) and Lauer et al. (2007a) had used the Nuker model to measure mass deficits that are up to an order of magnitude larger than those obtained here. As detailed in Trujillo et al. (2004) and Dullo & Graham (2012), this discrepancy arises in part from the differences in the estimated core sizes from the two models. While the Nuker model break radii are up to 3 times larger than the core-Sérsic model break radii, due to the Nuker model fitting a power-law to each galaxy’s outer curved Sérsic profile (Graham et al. 2003), the core-Sérsic break radii agree with model-independent core sizes where the negative logarithmic slope of the light profile equals 0.5 (Dullo & Graham 2012).

More recently, Kormendy et al. (2009) fit Sérsic models to core-Sérsic galaxy light profiles and tried to quantify

the core from a visual inspection, rather than using the core-Sérsic model in an objective analysis. They report large break radii and mass deficits $M_{\text{def}} \sim 10 - 20 M_{\text{BH}}$. In an effort to reconcile these large deficits, they speculated that they may be due to recoiled black holes, which might enhance the core depletion following their repetitive core passages (Boylan-Kolchin et al. 2004; Gaulandris & Merritt 2008); cf. also Postman et al. (2012) for a similar reasoning. If this mechanism always occurred, then the lower $M_{\text{def}}/M_{\text{BH}}$ ratios in Dullo & Graham (2012) for elliptical galaxies would suggest that the effective number of major mergers is less than one, i.e. only a minor merger is required. However given the near-linear relation between black hole mass and host spheroid mass, and luminosity, for core-Sérsic galaxies (Graham 2012; Graham & Scott 2012) this scenario is unlikely. At least for the elliptical core-Sérsic galaxies, which are the dominant population among the known core-Sérsic galaxies, this linear black hole-galaxy mass scaling relation readily arises from the self addition of comparable mass systems, not minor mergers.

6. DISCUSSION

6.1. Formation of core-Sérsic lenticular galaxies

As noted above, the central stellar mass deficits for the ‘core-Sérsic’ lenticular galaxies are found to be $M_{\text{def}} \sim 0.5 - 2 M_{\text{BH}}$ (Fig.4). By comparing these mass deficits with the results of Merritt (2006), one would conclude that the bulges of core-Sérsic S0s have experienced the equivalent of a few ‘dry’ major merger events. Deviations from this rule may however exist. For example, substantial black hole recoiling events would lower this figure of a few, while ‘loss cone’ re-filling through wet mergers and the production of new stars would allow scope for an increased number of mergers. This latter scenario is unlikely given, in general, the red colours of the galaxies’ bulges. However, Carter et al. (2011) have found $FUV - NUV$ colour gradients in several core-Sérsic galaxies which seem to be inconsistent with the major, dry merger scenario detailed in Faber et al. (1997). Also, the globular cluster specific frequencies of some intermediate luminosity ellipticals are found to be systematically lower than the ones in bright, core-Sérsic elliptical galaxies (Harris & van den Bergh 1981; van den Bergh 1982). This may reflect that core galaxy formation may not involve dry merger events, because such mergers are thought to be inefficient at creating new globular clusters.

Although not (yet) popular, various studies have proposed alternative mechanisms for generating cores in luminous galaxies. For example, N-body simulations by Nipoti et al. (2006) revealed that dissipationless collapses in preexisting dark matter haloes would naturally produce galaxies which resemble ellipticals galaxies with depleted cores. These galaxies may also exist at $z = 1.5$ to 2, however, it is unclear how these cores are protected against infalling high-density satellites in the absence of a central massive black hole. While the bulges of today’s S0s do not all possess partially depleted cores, this does not exclude today’s Sérsic bulges from having existed at $z = 1.5$ to 2. Indeed, as shown by MacArthur et al. (2009, and the references in Graham 2013) the bulk

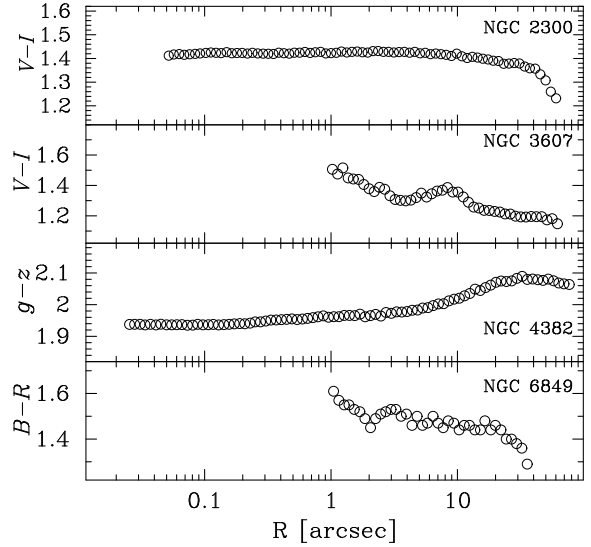


FIG. 5.— Radial colour profiles for four of the five lenticular galaxies listed in Table 2. Colour information is not available for NGC 507. The inner $R \lesssim 1''$ profile of NGC 3607 is excluded due to possible dust contamination. For NGC 6849, the $B - R$ color profile is derived using the published surface brightness profiles presented in Reda et al. (2004).

of most bulges’ stars are sufficiently old to have existed then.

Using numerical simulations, Goerdt et al. (2010) showed that the energy transferred from sinking massive objects can generate cores that are up to 3 kpc in sizes. Similarly, Martizzi et al. (2012a, see also Martizzi et al. 2012b) used 500 pc resolution simulations and concluded that the combined effects of AGN feedback and inspiralling massive black holes create cores in luminous elliptical galaxies that are up to 8 - 10 kpc in sizes. However, these overly large cores reported by Goerdt et al. (2010) and Martizzi et al. (2012a) are in general incompatible with the majority of $\lesssim 0.5$ kpc cores observed in real galaxies (e.g., Trujillo et al. 2004; Richings et al. 2011; Dullo & Graham 2012).

One can envisage that a core in a core-Sérsic S0 galaxy may be created through the ‘dry’ intermediate-mass merger (with mass ratio 1:4 to 1:7) of an S0 galaxy with a smaller elliptical galaxy, such that the disk is not destroyed but the bulge grows while the black hole binary created during the merger ejects stars from the inner regions of the bulge. Eliche-Moral et al. (2012; see also Bekki 1998; Bournaud et al. 2005) has recently explored this merger scenario and concluded that ‘dry’ intermediate-mass mergers can give rise to remnants that are both photometrically and kinematically compatible with the observed S0s. It should, however, be noted that these studies did not explore the actual nuclear structure of the merger remnants. Another possibility may be minor disk galaxy mergers which result in a rotating, disk merger remnant (Burkert & Naab 2005; Jesseit et al. 2005). Core-Sérsic S0 galaxies might also or instead be assembled via an inside-out mechanism: an early major merger might create an elliptical galaxy with a depleted core, around which a disk is subsequently built up over time via ‘dry’ minor mergers and/or smooth cold gas accretion. The assumption here is that the accretion process is very gentle and slow, enabling the cold gas to assemble into a star-forming disk (e.g., Steinmetz &

TABLE 3
CORE-SÉRSIC GALAXY DATA.

Galaxy	M/L_V	$\log(M_*/M_\odot)$	R_e (kpc)	$\log(L_{def}/L_{\odot,V})$	$\log(M_{def}/M_\odot)$	$\log(M_{BH}/M_\odot)$
(1)	(2)	(3)	(4)	(5)	(6)	(7)
NGC 0507	5.5	11.70	1.65	8.34	9.08	9.22 ± 0.39
NGC 2300	5.0	11.16	1.02	7.81	8.51	8.86 ± 0.39
NGC 3607	5.7	11.31	0.84	—	—	—
NGC 3706	5.2	11.60	9.18	8.30	9.01	8.93 ± 0.39
NGC 4382	2.6	10.90	0.99	7.68	8.09	7.98 ± 0.38
NGC 6849	2.4	11.32	2.98	7.97	8.35	8.04 ± 0.43

Notes.—Col. (1) Galaxy name. Col. (2) V -band stellar mass-to-light (M/L) ratio. Col. (3) Stellar mass of the bulge obtained using the bulge magnitude (Table 1) and the stellar mass-to-light (M/L) ratio (col. 2) (for the elliptical galaxy NGC 3706 the contribution of the galaxy’s nuclear stellar ring has not been subtracted). Col. (4) Major-axis half-light radius of the bulge. Col. (5) Central luminosity deficit in terms of V -band solar luminosity. Col. (6) Central stellar mass deficit obtained using col. (2) and col. (5). Col. (7) SMBH mass predicted from the $M - \sigma$ relation presented in Graham et al. (2011). We use Eq. 4 from Graham et al. (2011) and the σ -values in Table 1 and a 10% uncertainty on σ to estimate the error on SMBH mass. We adopt a barred morphology to estimate the mass of the black hole in NGC 6849.

Navarro 2002; Birnboim & Dekel 2003; Kereš et al. 2005) and also preventing it from falling towards the centers of the bulges, which otherwise would fuel a central burst of star formation and replenish the depleted cores.

These later core-Sérsic galaxy formation scenarios, each involving merger events, may be in agreement with the properties of our high luminosity S0 bulges. This is in contrast to models that produce S0s by fading the disks of spiral galaxies through processes such as ram pressure stripping (e.g., Gunn & Gott 1972)—which is not to say that such processing does not additionally occur.

6.2. *Bulges of today’s S0s versus compact high redshift galaxies*

Recent observations have revealed that the sizes of compact massive galaxies at redshift of $z \sim 1.5$ to 2 (having effective radii $R_e \lesssim 2$ kpc) are up to a factor of ~ 5 smaller than the present day elliptical galaxies of comparable stellar mass (Daddi et al. 2005; Trujillo et al. 2006; Damjanov et al. 2009; Saracco et al. 2011; Szomoru et al. 2012, and references therein). While today’s elliptical galaxies are widely regarded as the descendants of these compact high redshift galaxies (e.g., Hopkins et al. 2009), Graham (2013, his Fig. 1) showed that massive local disk galaxies can also be alternative candidates given the high stellar density and compactness of their bulges. Comparing the properties of our massive present day bulges with compact high redshift galaxies, we plot the size-mass (Fig. 6a) and size-(Sérsic index) (Fig. 6b) diagrams for a sample of 106 galaxies. 101 of these objects are compact massive quiescent galaxies at redshift $z = 0.2$ to 2.7 taken from Damjanov et al. (2011, selected from their Table 2), while five are the bulges from local S0s (Table 2 and 3). This figure clearly shows that the location of the bulges of our five core-Sérsic S0s coincides with that of the high-redshift compact galaxies in both the $R_e - M_*$ and $R_e - n$ diagrams.

This overlap suggests that the compact high redshift galaxies are the progenitors of (the bulges of) massive present day S0s (e.g., Dutton et al. 2012; Graham et al. 2013). Indeed, the inside-out growth mechanism described at the end of Section 6.1, which could drive the build up of the core-Sérsic S0s (Section 6.3), would also eliminate the difficulties encountered in trying to explain the size evolution of these compact high redshift galaxies

into much larger, modern day elliptical galaxies. Large elliptical galaxies already exist at $z \approx 1.5$ to 2 (e.g., Bruce et al. 2012). We further note that van der Wel. (2011, see also Chevance et al. 2012) wrote that the majority of compact high redshift galaxies have small undeveloped disks. In addition, Poggianti et al. (2012) found that 4.4% of their total low redshift galaxy population had sizes and mass densities comparable to the compact, massive high redshift galaxies, with 70% of these compact low redshift galaxies found to be S0s. Given the results in Graham (2013, his Fig. 1), a comparison of local S0 galaxy “bulge” sizes and densities, rather than the entire “galaxy” sizes and densities, should yield a higher percentage match. It seems plausible that minor mergers and cold gas accretion (e.g., Conselice et al. 2012), in a preferred plane due to known cosmological streaming/feeding paths, may transform some of the compact high redshift galaxies into modern S0s by the creation of a younger surrounding disk. This process eliminates the difficulties that arise when trying to evolve the compact high- z galaxies into local elliptical galaxies, such as the shortage of satellites required to produce the necessary expansion via many minor mergers (Trujillo et al. 2012). It is also consistent with cosmological models (e.g., Steinmetz & Navarro 2002), and explains many properties of early-type galaxies.

6.3. *The role of galaxy environment*

Several studies have highlighted that environment plays a major role in the formation of S0 galaxies (e.g., Dressler 1980; Dressler et al. 1997; Couch et al. 1998; Fasano et al. 2000; Poggianti et al. 2009; Wilman et al. 2009; Just et al. 2010; Bekki & Couch 2011). Three of our five S0 galaxies (NGC 507, NGC 2300 and NGC 3607) reside in X-ray bright galaxy groups, while NGC 6849 is an isolated galaxy, and NGC 4382 is a member of the Virgo cluster.

NGC 6849, the isolated core-Sérsic lenticular galaxy, may have had its bulge built through an early violent ‘dry’ major merger, while subsequent late accretion of gas and stars built up its disk—the picture in Graham (2013), see also Conselice et al. (2012). This hierarchical inside-out growth scenario is supported by its radial colour profile plotted in Fig. 5. The $B - R$ colour gradient reveals that the galaxy becomes progressively bluer

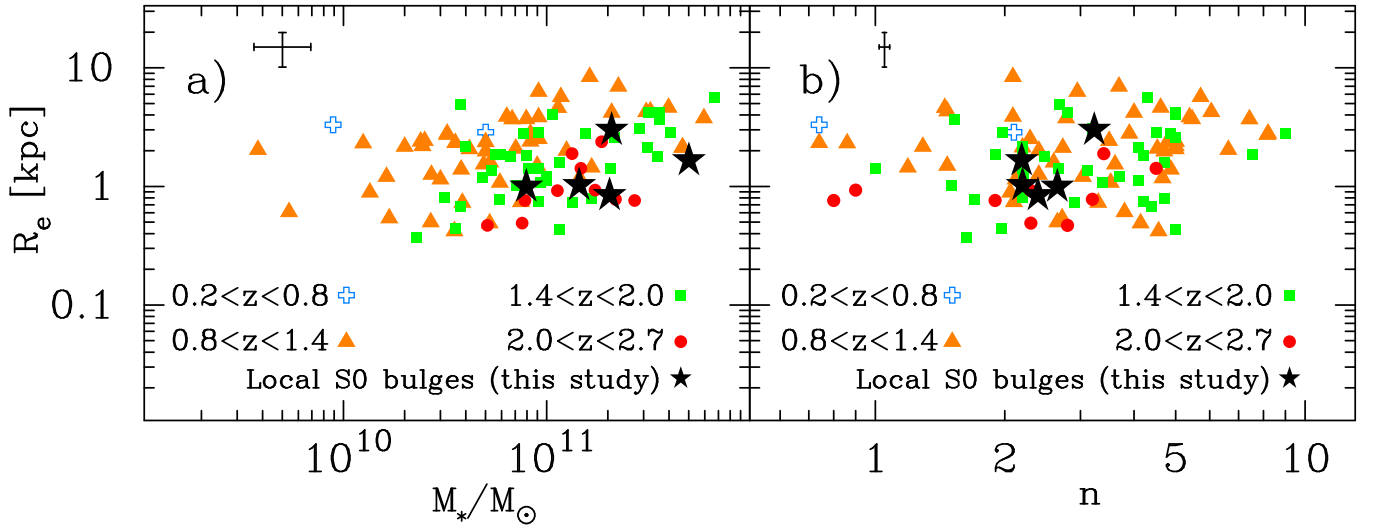


FIG. 6.— Major-axis effective radius R_e plotted against (a) stellar mass M_* , and (b) Sérsic index n for a sample of 106 galaxies. 101 of these objects are massive compact galaxies, in the redshift range $0.2 < z < 2.7$, published by Damjanov et al. (2011, their Table 2 excluding galaxies (i) with no reported n values, (ii) fitted with the de Vaucouleurs ($R^{1/4}$) model, and (iii) modelled by setting n to some constant value). The remaining five are local S0 bulges from this study (Table 2 and 3). Median uncertainty from Damjanov et al. (2011) for the 101 galaxies is shown by the error bar at the top of each panel.

towards larger radii ($\gtrsim 10''$) where the disk dominates. Arnold et al. (2011) proposed such a two phase assembly mechanism to explain the isolated field galaxy NGC 3115 (except for its dwarf companion) based on their analysis of its kinematics and metallicity. Reda et al. (2004) also found that mergers are a dominant formation path to forming some isolated early-type galaxies. In passing we note that van den Bergh (2009) alternatively suggested that disk gas ejection by AGN might be a dominant process that transforms isolated spirals galaxies into S0s. While by itself this process does not appear capable of generating a depleted stellar core in galaxies, it may have transformed some spiral galaxies into lenticular galaxies.

The ‘dry’ major merger scenario for the bulges of bright lenticular galaxies in groups may be naturally consistent with the observed morphology density relation for the galaxy groups. Studies have shown that galaxy-galaxy interaction and merging play an important role in transforming group spirals into S0s and giving the observed S0 fractions in groups (e.g., Postman & Geller 1984; Helsdon & Ponman 2003; Just et al. 2010; Bekki & Couch 2011). Our three X-ray bright group galaxies are the brightest central galaxies from their respective groups. As pointed by Helsdon & Ponman (2003 and references therein) these central S0 galaxies are assumed to be the byproducts of an earlier merger activity in the collapsing group core plus some recent merger and accretion events. Interestingly, as shown in Fig. 5, the outskirts of these galaxies (colour information was not available for NGC 507) are relatively bluer than their centers. This result further strengthens the view that bulges in luminous group S0s grow by mergers while their disks are gradually built and enhanced via latter gas accretion.

For NGC 4382, our fifth lenticular galaxy and the only cluster galaxy in our sample, our analysis of its brightness profile and thus the mass deficit (Figs. 3 and 4) suggests a ‘dry’ merger event as a formation path. In contrast, processes such as ram pressure stripping (Gunn &

Gott 1972; Quilis et al. 2000), galaxy harassment (Moore et al. 1996) and strangulation (Larson 1980; Bekki et al. 2002) are often noted as plausible formation mechanisms for cluster lenticular galaxies, rather than galaxy mergers, due to the high cluster velocity dispersion and high intracluster medium density. We do not deny these mechanisms, only that they alone cannot account for partially depleted cores. For example, Vollmer et al. (2008a, 2008b) present wonderful observational evidence of the ram pressure stripped Virgo spiral galaxies NGC 4501 and NGC 4522, while Merluzzi et al. (2012) describe in detail the stripping process of a galaxy in Abell 3558. The merger event in NGC 4382’s past may have occurred prior to it entering the cluster. Coupling N-body simulations with a semi-analytic formation model, Okamoto & Nagashima (2001) also reported that the fractions of cluster S0 galaxies produced by major mergers are significantly smaller than the observed fractions. In contrast, Bekki (1998) proposed unequal galaxy merging between two spirals as a dominant formation origin for cluster lenticular galaxies (see also Burkert & Naab 2005 and Jesseit et al. 2005). NGC 4382 is situated in the outskirts of the Virgo cluster, a location where mergers are likely to occur, and it displays stellar shells in its image (Schweizer & Seitzer 1992). These appear to suggest that NGC 4382 might have a merger related origin (although see Chung et al. 2009). The $g - z = 1.95$ bulge colour of NGC 4382 (Fig. 5) is however bluer than the typical $g - z = 1.56$ (AB mag) colour quoted for ellipticals (Fukugita et al. 1995). If the core in NGC 4382 was formed from the inspiral of supermassive black holes in a relatively gas-free merger event, then the progenitor stars which make the bulge were not old, suggestive of ongoing core formation in some lenticular galaxies rather than all being formed at redshifts beyond 1.5 to 2 prior to the subsequent accretion of a disk.

7. CONCLUSIONS

We have used the IRAF ELLIPSE task to derive the major-axis surface brightness profiles and isophotal parameters for six early-type galaxies observed with the high-resolution *HST* WFPC2 and ACS cameras. While one of these turned out to be an elliptical galaxy, which we modelled with a core-Sérsic profile, we have modeled the surface brightness profiles of the remaining five lenticular galaxies using a core-Sérsic model for the bulge plus an exponential model for the disk. This is the first time this has been done for disk galaxies with depleted cores. In our analysis, we have additionally accounted for the bar component in one of these disk galaxies by using the Ferrers (1877) function. Our primary conclusions are as follows:

1. The core-Sérsic bulge plus exponential disk model gives an accurate description to core-Sérsic lenticular galaxy light profiles. The rms residual scatter of the fits are $\lesssim 0.05$ mag arcsec $^{-2}$.
2. The Sérsic index n is ~ 3 for the bulges of our core-Sérsic lenticular galaxies, whereas $n \gtrsim 3$ for the brighter core-Sérsic elliptical galaxies in Dullo & Graham (2012).
3. The core ‘break radii’ range from 24 to 102 pc.
4. We have measured central stellar mass deficits in four of the luminous “core-Sérsic” lenticular galaxies, finding $M_{\text{def}} \sim 0.5 - 2 M_{\text{BH}}$, in agreement with previous core-Sérsic analysis of elliptical galaxies. (NGC 3607 was excluded because its dusty nuclear spiral compro-

mises the recovery of its core parameters.)

5. Our results tentatively suggest that, regardless of their environments, core-Sérsic lenticular galaxies could be assembled in two stages: an earlier violent ‘dry’ major merger process involving massive black holes, which forms the bulge component, followed by subsequent disk formation through minor mergers and/or very gentle cold gas accretion about a preferred plane. Dry intermediate-mass ratio mergers of S0s with smaller BH-hosting ellipticals could also account for the buildup of some core-Sérsic S0s.

6. The location of the bulges of our five S0 galaxies, including the S0 NGC 3607 possibly with out a depleted core, in the mass-size and mass-(Sérsic index) diagram coincides with that of the compact early-type galaxies seen at redshift of $z \sim 0.2$ to 2.7. This could be an indication that today’s massive bulges may be descendants of the compact high redshift early-type galaxies.

8. ACKNOWLEDGMENTS

This research was supported under the Australian Research Councils funding scheme (DP110103509 and FT110100263). This research has made use of the NASA/IPAC Extragalactic Database (NED) which is operated by the Jet Propulsion Laboratory, California Institute of Technology, under contract with the National Aeronautics and Space Administration. We are grateful to Juan P. Madrid for his help with IRAF.

REFERENCES

- Afanasiev, V. L., & Sil’chenko, O. K. 2007, *Astron. Astrophys. Trans.*, 26, 311
- Andredakis, Y. C., Peletier, R. F., & Balcells, M. 1995, *MNRAS*, 275, 874
- Arnold, J. A., Romanowsky, A. J., Brodie, J. P., et al. 2011, *ApJ*, 736, L26
- Barnes, J. E., Hernquist, L., 1992, *ARA&A*, 30, 705
- Begelman, M. C., Blandford, R. D., & Rees, M. J. 1980, *Nature*, 287, 307
- Bell, E.F., Wolf C., Meisenheimer, K., et al. 2004, *ApJ*, 608, 752
- Bell, E. F. et al., 2006, *ApJ*, 640, 241
- Bekki, K. 1998, *ApJL*, 502, 133
- Bekki, K., Couch, W. J., & Shioya, Y. 2002, *ApJ*, 577, 651
- Bekki, K., & Couch, W. J. 2011, *MNRAS*, 415, 1783
- Bekki, K. & Graham, A. W. 2010, *ApJ*, 714, L313
- Bender, R., Doebereiner, S., Moellenhoff C. 1988, *A&AS*, 74, 385
- Bezanson, R., van Dokkum, P., & Franx M. 2012, *ApJ*, 760, 62
- Blakeslee, J. P., Lucy, J. R., Tonry, J. L., Hudson, M. J., Narayanan, V. K., Harris, B. J., 2002, *MNRAS*, 330, 443
- Birnboim, Y., Dekel, A. 2003, *MNRAS*, 345, 349
- Bournaud, F., Jog, C. J., & Combes, F. 2005, *A&A*, 437, 69
- Boylan-Kolchin, M., Ma C.-P., 2007, *MNRAS*, 374, 1227
- Boylan-Kolchin, M., Ma C., Quataert, E., 2004, *ApJ*, 613, L37
- Bluck, A. F. L., Conselice, C. J., Buitrago, F., Grützbauch, R., Hoyos C., Mortlock, A., Bauer, A. E., 2012, *ApJ*, 747, 34
- Bruce, V. A., Dunlop, J. S., Cirasuolo, M., et al. 2012, *MNRAS*, 427, 1666
- Burkert, A., & Naab, T. 2005, *MNRAS*, 363, 597
- Byun, Y.-I., et al. 1996, *AJ*, 111, 1889
- Caon N., Capaccioli M., D’Onofrio, M. 1993, *MNRAS*, 265, 1013
- Cappellari, M. et al., 2007, *MNRAS*, 379, 418
- Cappellari, M., McDermid, R. M., 2005, *Class. Quantum Grav.*, 22, 347
- Carter, D. 1978, *MNRAS*, 182, 797
- Carter, D. 1987, *ApJ*, 312, 514
- Carter, D., Pass S., Kennedy J., Karick A.M., Smith R.J. 2011, *MNRAS*, 414, 341
- Cattaneo, A. et al., 2009, *Nat*, 460, 213
- Chevance, M., Weijmans, A., Damjanov, I. et al., 2012, *ApJ*, 754, 24
- Chung A., van Gorkom J. H., Kenney J. D. P., Crowl H., Vollmer B., 2009, *AJ*, 138, 1741
- Conselice, C. J., et al, arXiv:1206.6995
- Couch, W. J., Barger, A. J., Smail, I., Ellis, R. S., Sharples, R. M., 1998, *ApJ*, 430, 121
- Cox, T. J., Jonsson, P., Primack, J. R., & Somerville, R. S. 2006, *MNRAS*, 373, 1013
- Chung, A., van Gorkom, J. H., Kenney, J. D. P., Crowl, H., & Vollmer, B. 2009, *AJ*, 138, 1741
- Daddi, E., Renzini, A., Pirzkal, N., et al. 2005, *ApJ*, 626, 680
- Damjanov, I., Abraham, R. G., & Glazebrook, K. et al. 2011, *ApJ*, 739, L44
- Damjanov, I., McCarthy, P. J., & Abraham, R. G. et al. 2009, *ApJ*, 695, 101
- Davies, R.L., Efstathiou, G., Fall, S.M., Illingworth, G., Schechter, P.L. 1983, *ApJ*, 266, 41
- Desai, V., et al., 2007, *ApJ*, 660, 1151
- de Souza, R. E., Gadotti, D. A., dos Anjos, S., 2004, *ApJS*, 153, 411
- de Vaucouleurs, G., 1948, *Ann. d’Astrophys.*, 11, 247
- de Vaucouleurs, G., de Vaucouleurs A., Corwin H. G., Jr., et al. 1991, *Third Reference Catalogue of Bright Galaxies* (Berlin: Springer)
- Dhar, B. K., & Williams L. L. R., arXiv:1112.3120
- Dressler, A., 1980, *ApJ*, 236, 351
- Dressler, A., Oemler A., Couch W. J., Smail I., Ellis R. S., Barger A., Butcher H., Poggianti B. M., Sharples R. M., 1997, *ApJ*, 490, 577
- Driver, S. P., Popescu, C. C., Tuffs, R. J., Graham, A. W., Liske, J., Baldry, I., 2008, *ApJ*, 678, L101
- Dullo, B. T., & Graham, A. W., *ApJ*, 755, 163
- Dutton, A. A., Treu, T., Brewer, B. J., et al. 2012, *MNRAS*, submitted, arXiv:1206.4310
- Ebisuzaki, T., Makino, J., & Okumura, S. K. 1991, *Nature*, 354, 212
- Eliche-Moral, M. C., Gonzale-Garcia, A. C., Aguerri, J. A., et al., arXiv:1209.0782
- Emsellem, E., Cappellari, M., Krajnović, D., et al. 2007, *MNRAS*, 379, 401
- Emsellem, E., Cappellari, M., Krajnović, D., et al. 2011, *MNRAS*, 414, 888

- Emsellem, E., Cappellari, M., Peletier, R. F., et al. 2004, *MNRAS*, 352, 721
- Faber, S. M., et al. 1997, *AJ*, 114, 1771
- Fasano, G., Poggianti, B. M., Couch, W. J., Bettoni, D., Kjægaard, P., Moles, M., 2000, *ApJ*, 542, 673
- Ferrarese, L., et al. 2006, *ApJS*, 164, 334
- Ferrarese, L., Ford H., 2005, *Space Sci. Rev.*, 116, 523
- Ferrarese, L., van den Bosch, F. C., Ford, H. C., Jaffe, W., & O'Connell, R. W. 1994, *AJ*, 108, 1598
- Ferrers, N.M. 1877, *Quart. J. Pure Appl. Math.*, 14, 1
- Forbes, D.A., Spitler, L.R., Strader, J., et al. 2011, *MNRAS*, 413, 2943
- Ford, H. C., Bartko, F., Bely, P. Y., et al. 1998, *Proc. SPIE*, 3356, 234
- Goerdt, T., Moore, B., Read, J. I., Stadel, J., 2010, *ApJ*, 725, 1707
- Governato, F., Brook, C. B., Brooks, A. M., Mayer, L., Willman, B., Jonsson P., Stilp, A. M., Pope, L., Christensen, C., Wadsley, J., Quinn T., 2009, *MNRAS*, 398, 312
- Graham, A. W., 2001, *AJ*, 121, 820
- Graham, A. W., 2004, *ApJ*, 613, L33
- Graham, A. W., 2007, *MNRAS*, 379, 711
- Graham, A. W., 2012, *ApJ*, 746, 113
- Graham, A. W., 2013, to appear in 'Planets, Stars and Stellar Systems'. Springer, Berlin, preprint (arXiv:1108.0997)
- Graham, A. W., Colless, M. M., Busarello, G., Zaggia, S., & Longo, G. 1998, *A&AS*, 133, 325
- Graham, A. W., & Driver S.P. 2005, *Publ. Astron. Soc. Australia*, 22, 118
- Graham, A. W., Erwin P., Trujillo I., & Asensio Ramos A. 2003, *AJ*, 125, 2951
- Graham, A. W., & Guzmán, R. 2003, *AJ*, 125, 2936
- Graham, A. W., Onken, C.A., Athanassoula, E., & Combes, F. 2011, *MNRAS*, 412, 2211
- Graham, A. W., & Scott, N. 2013, *ApJ*, 764, 151
- Graham, A. W., Spitler, L. R., 2009, *MNRAS*, 397, 2148
- Graham, A. W., Trujillo, I., Caon, N., 2001, *AJ*, 122, 1707
- Graham, A. W., & Worley, C.C., 2008, *MNRAS*, 388, 1708
- Gualandris, A., Merritt, D., 2008, *ApJ*, 678, 780
- Gualandris, A., & Merritt, D. 2012, *ApJ*, 744, 74
- Gültekin, K., Richstone, D. O., Gebhardt, K., et al. 2009, *ApJ*, 695, 1577
- Gültekin K., Richstone D. O., Gebhardt K., et al. 2011, *ApJ*, 741, 38
- Gunn, J. E., Gott, J. R. III., 1972, *ApJ*, 176, 1
- Gutiérrez, L., Erwin, P., Aladro, R., & Beckman, J. E. 2011, *AJ*, 142, 145
- Harris, W.E., van den Bergh, S. 1981, *AJ*, 86, 1627
- Helsdon, S. F., & Ponman, T. J. 2003, *MNRAS*, 339, L29
- Holtzman, J. A., Burrows, C. J., Casertano, S., Hester, J. J., Trauger, J. T., Watson, A. M., Worthey, G., 1995, *PASP*, 107, 1065
- Hopkins, P. F., Bundy, K., Murray, N., Quataert, E., Lauer, T. R., Ma C.-P., 2009, *MNRAS*, 398, 898
- Hopkins, P. F., & Hernquist, L. 2010, *MNRAS*, 407, 447
- Hubble, E. 1929, *Proceedings of the National Academy of Science*, 15, 168
- Hubble, E.P. 1936, *The Realm of the Nebulae*, by E.P. Hubble, New Haven: Yale University Press
- Huchtmeier, W. K., 1994, *A&A*, 286, 389
- Hyde, J. B., Bernardi M., Fritz A., Sheth R. K., Nichol R. C., 2008, *MNRAS*, 391, 1559
- Jaffe, W., Ford H. C., O'Connell R. W., van den Bosch F. C., & Ferrarese L. 1994, *AJ*, 108, 1567
- Jeans, J.H. 1928, *Astronomy & Cosmogony*, (Cambridge: Cambridge University Press), p.332
- Jedrzejewski, R. I., 1987, *MNRAS*, 226, 747
- Jesseit, R., Naab, T., & Burkert, A. 2005, *MNRAS*, 360, 1185
- Just, D. W., Zaritsky D., Sand D. J., Desai V., & Rudnick G. 2010, *ApJ*, 711, 192
- Kandrup, H. E., Sideris I. V., Terzić B., Bohn C. L., 2003, *ApJ*, 597, 111
- Kauffmann, G., & Haehnelt, M. 2000, *MNRAS*, 311, 576
- Kawata, D. & Mulchaey J. S. 2008, *ApJ*, 672, L103
- Kereš, D., Katz, N., Weinberg, D. H., & Davé, R. 2005, *MNRAS*, 363, 2
- Khochfar, S., Burkert, A., 2001, *ApJ*, 561, 517
- Kim, T., Sheth, K., Hinz, J. L., et al. 2012, *ApJ*, 753, 43
- Kormendy, J., & Bender, R. 2009, *ApJ*, 691, L142
- Kormendy, J., Fisher, D.B., Cornell, M.E., Bender, R. 2009, *ApJS*, 182, 216
- Krajinović, D., Cappellari, M., de Zeeuw, P. T., & Copin, Y. 2006, *MNRAS*, 366, 787
- Kulkarni, G. & Loeb, A. 2012, *MNRAS*, 422, 1306
- Larson, R. B., Tinsley, B. M., Caldwell, C. N., 1980, *ApJ*, 237, 692
- Lauer, T. R. 2012, arXiv:1209.4357
- Lauer, T. et al., 2002, *AJ*, 124, 1975
- Lauer, T. R., Ajhar, E. A., Byun, Y.-I., et al. 1995, *AJ*, 110, 2622
- Lauer, T. R., et al. 2005, *AJ*, 129, 2138
- Lauer, T. R., et al., 2007a, *ApJ*, 662, 808
- Lauer, T. R., et al., 2007b, *ApJ*, 664, 226
- Laurikainen, E., Salo H., Buta R., Knapen J. H., & Comerón S. 2010, *MNRAS*, 405, 1089
- Li, Z.-Y., Ho, L. C., Barth, A. J., & Peng, C. Y. 2011, *ApJS*, 197, 22
- Longo, G., Zaggia, S. R., Busarello, G., & Richter, G. 1994, *A&AS*, 105, 433
- MacArthur, L.A., González, J.J., Courteau, S. 2009, *MNRAS*, 395, 28
- Magorrian, J., et al. 1998, *AJ*, 115, 2285
- Man, A. W. S., Toft, S., Zirm, A. W., Wuyts, S., van der Wel, A., 2012, *ApJ*, 744, 85
- Martizzi, D., Teyssier R., & Moore B. 2012a, *MNRAS*, 420, 2859
- Martizzi, D., Teyssier R., & Moore B., 2012b, arXiv:1211.2648
- Meert, A., Vikram, V., & Bernardi, M. 2012, arXiv:1211.6123
- Merluzzi, P., Busarello, G., Dopita, M.A., et al. 2012, *MNRAS*, arXiv:1211.6532
- Merritt, D., 2006, *ApJ*, 648, 976
- Michard, R., & Marchal, J. 1993, *A&AS*, 98, 29
- Milosavljević, M., & Merritt, D. 2001, *ApJ*, 563, 34
- Milosavljević, M., Merritt, D., Rest A., & van den Bosch, F. C. 2002, *MNRAS*, 331, L51
- Moore, B., Katz, N., Lake, G., Dressler, A., Oemler, A., 1996, *Nature*, 379, 613
- Mulchaey, J. S., Davis, D. S., Mushotzky, R. F., & Burstein, D. 1993, *ApJ*, 404, L9
- Nieto, J.-P., & Bender, R. 1989, *A&A*, 215, 266
- Nipoti, C., Londrillo, P., Ciotti, L., 2006, *MNRAS*, 370, 681
- Okamoto, T., Nagashima, M., 2001, *ApJ*, 547, 109
- Paturel, G., Petit, C., Prugniel, P., Theureau, G., Rousseau, J., Brouty, M., Dubois P., Cambrésy, L., 2003, *A&A*, 412, 45
- Peletier, R.F., Davies, R.L., Illingworth, G.D., Davis, L.E., Cawson, M. 1990, *AJ*, 100, 1091
- Peirani, S., Kay, S., & Silk, J. 2008, *A&A*, 479, 123
- Pichon, C., Pogossyan, D., Kimm, T., et al. 2011, *MNRAS*, 418, 2493
- Pinkney, J., Gebhardt, K., Bender, R., et al. 2003, *ApJ*, 596, 903
- Poggianti, B. M., et al., 2009, *ApJL*, 697, 137
- Poggianti, B. M., et al., *ApJ*, arXiv:1211.1005
- Postman, M., et al., 2012, *ApJ*, arXiv:1205.3839
- Postman, M., & Geller, M. J. 1984, *ApJ*, 281, 95
- Quilis, V., Moore, B., & Bower, R. 2000, *Science*, 288, 1617
- Ravindranath, S., Ho, L. C., & Filippenko, A. V. 2002, *ApJ*, 566, 801
- Ravindranath, S., Ho, L. C., Peng, C. Y., Filippenko, A. V., & Sargent, W. L. W. 2001, *AJ*, 122, 653
- Reda, F. M., Forbes, D. A., Beasley, M. A., OSullivan, E. J., Goudfrooij, P., 2004, *MNRAS*, 354, 851
- Rest, A., van den Bosch, F. C., Jaffe, W., Tran, H., Tsvetanov, Z., Ford, H. C., Davies, J., & Schafer, J. 2001, *AJ*, 121, 2431
- Richings, A. J., Uttley, P., & Kröding, E., 2011, *MNRAS*, tmp, 759
- Richstone, D., et al. 1998, *Nature*, 395, 14
- Sales, L. V., Navarro, J. F., Theuns, T., Schaye, J., White, S. D. M., Frenk C. S., Crain, R. A., Dalla Vecchia, C., 2012, *MNRAS*, 423, 1544
- Saracco, P., Longhetti, M., & Gargiulo, A., 2011, *MNRAS*, 412, 2707
- Saraiva, M. F., Ferrari, F., Pastoriza, M. G., 1999, *A&A*, 350, 339
- Schweizer, F., & Seitzer, P. 1992, *AJ*, 104, 1039
- Sérsic, J. L. 1963, *Boletín de la Asociación Argentina de Astronomía*, 6, 41
- Sesana, A., 2010, *ApJ*, 719, 851
- Silchenko, O. K., Moiseev A. V., & Shulga A. P. 2010, *AJ*, 140, 1462
- Sirianni, M., Jee, M. J., Benítez, N., et al. 2005, *PASP*, 117, 1049
- Steinmetz, M., Navarro, J. F., 2002, *New Astronomy*, 7, 155
- Szomoru, D., Franx, M., & van Dokkum, P. G. 2012, *ApJ*, 749, 121

Terashima, Y., Ho, L. C., & Ptak, A. F. 2000, ApJ, 539, 161
 Tonry, J. L., et al., 2001, ApJ, 546, 681
 Toomre, A., & Toomre, J. 1972, ApJ, 178, 623
 Trujillo, I. 2012, arXiv:1211.3771
 Trujillo, I., Erwin, P., Asensio Ramos, A., & Graham, A. W. 2004, AJ, 127, 1917
 Trujillo, I., Feulner, G., Goranova, Y., et al. 2006, MNRAS, 373, L36
 Turner, M. L., Côté, P., Ferrarese, L., et al., arXiv:1208.0338
 van den Bergh, S., 2009, ApJ, 702, 1502

van den Bergh, S., 1982, PASP, 94, 459
 van der Wel, A., Rix H.-W., & Wuyts S. et al. 2011, ApJ, 730, 38
 Vollmer, B., Braine, J., Pappalardo, C., & Hily-Blant, P. 2008b, A&A, 491, 455
 Vollmer, B., Soida, M., Chung, A., et al. 2008a, A&A, 483, 89
 Wilman, D. J., Oemler, A., Mulchaey, J. S., McGee S. L., Balogh M. L., & Bower, R. G. 2009, ApJ, 692, 298
 White, S. D. M., Rees, M. J., 1978, MNRAS, 183, 34
 Xu, C. K., Zhao, Y., Scoville, N., et al. 2012, ApJ, 747, 85
 Yu, Q., 2002, MNRAS, 331, 935

9. APPENDIX A

9.1. Notes on individual galaxies

In this section we review several relevant features associated with each galaxy in our sample. We comment on the X-ray properties as this will be relevant to our later discussion about formation scenarios and environment.

9.1.1. NGC 507

NGC 507 is the brightest galaxy in the nearby, poor NGC 507 group; it is also one of the brightest known X-ray early-type galaxies. Laurikainen et al. (2010) found evidence of a weak bar in their K_s -band image. However, they fitted a Sérsic bulge plus an exponential disk to their deep sub-arcsec resolution K_s -band data because the bar was too weak to be included in the fit. Our high-resolution *HST*/F555W surface brightness profile for this galaxy is well fit by the core-Sérsic bulge + exponential disk model with an rms residual of $0.027 \text{ mag arcsec}^{-2}$ (Fig. 3).

9.1.2. NGC 2300

NGC 2300 belongs to the poor NGC 2300 group. Mulchaey et al. (1993) reported the presence of hot diffuse intragroup gas close to NGC 2300 using *ROSAT*. Although several previous studies (e.g., Huchtmeier 1994, Sandage & Bedke 1994) have classified this galaxy as an elliptical, as shown in Fig. 3, the luminosity profile is well fit by the core-Sérsic bulge + exponential disk model (see also Laurikainen et al. 2010 for their Sérsic + exponential fit to ground-based data that does not resolve the depleted core.)

9.1.3. NGC 3607

NGC 3607 is an X-ray luminous (e.g., Terashima et al. 2000), bright lenticular galaxy (e.g., de Vaucouleurs et al. 1991; Afanasiev & Silchenko 2007; Laurikainen et al. 2010; Gutiérrez et al. 2011; although it is classified as an elliptical in Gültekin et al. 2009) located in the Leo II group. It has a dust obscured central region as can be seen from the residual image in Appendix B, Fig. 8. We constructed an image model using the IRAF task BMODEL and subtracted it from the raw *V*-band image to obtain this residual image. The effect of this dusty nuclear spiral can also be seen in the position angle, ellipticity and isophote shape parameter (B_4) profiles (Fig. 2). In addition to using this to guide the careful dust masking procedure, performed prior to running ELLIPSE to obtain the *V*-band light profile beyond $1''$, we have analysed the galaxy's near-infrared *HST*/NICMOS F160W (*H*-band) image which is less affected by dust. As noted in Section 2, the inner ($R \lesssim 1''$) *V*-band profile of this galaxy, taken from Lauer et al. (2005), is derived from a PSF-deconvolved image. Therefore, the apparent $1''.31$ core of the *V*-band profile fit is most likely an artifact due to interference from the dusty nuclear spiral disk with the deconvolution routine (as noted already by Dullo & Graham 2012, and references therein).

9.1.4. NGC 3706

In agreement with the ground-based work by Laurikainen et al. (2010), the analysis of NGC 3706's *HST*/F555W light profile suggests that it is likely an elliptical galaxy rather than a lenticular galaxy. The unsharp-masked image (Appendix B, Fig. 8), the position angle twist, the disk and very flat ('pointy') nature of the isophotes from the ELLIPSE fit in the region $R = 0''.2 - 1''.0$ (Fig. 2) reveal the presence of an edge-on nuclear ring of stars in this galaxy (Lauer et al. 2002; Kandrup et al. 2003). We model the host galaxy light profile after excluding the region affected by this additional ring of star light (Fig. 3).

9.1.5. NGC 4382

NGC 4382 is a peculiar, fast rotating galaxy (Emsellem et al. 2007) in the Virgo cluster which is classified as an S0 in the RC3. Based on the photometry and brightness profile analysis, but not the rotational evidence, Kormendy et al. (2009) reported an absence of a large-scale stellar disk in this galaxy, and identified the extra light at large radii to be a feature associated with a recent merger (although see Chung et al. 2009), hence, they classified the galaxy as E2. In contrast, Laurikainen et al. (2011) have classified the galaxy as an S0 based on the detection of dispersed spiral arm segments, although they remained uncertain about the exponential nature of the disk light distribution. In Fig. 3, we show that the galaxy light profile is indeed well fit by the core-Sérsic bulge + exponential disk model with an rms residual of only $0.016 \text{ mag arcsec}^{-2}$. This galaxy has positive B_4 values, i.e. disk isophotes where $R > 1''$. We also note that we measure the galaxy's bulge-to-disk (B/D) flux ratio to be ~ 0.67 (B/T=0.40), revealing the existence of an appreciable fraction of the galaxy light in the large-scale disk. Dullo & Graham (2012, their Fig. 7) show how this large-scale disk results in a different "galaxy" Sérsic index, from the single-component fit in Ferrarese et al. (2006), compared to the "bulge" Sérsic index. Not fitting for the outer disk results in a 'galaxy' Sérsic index which is larger than the "bulge" Sérsic index and thus over-predicts the central mass deficit.

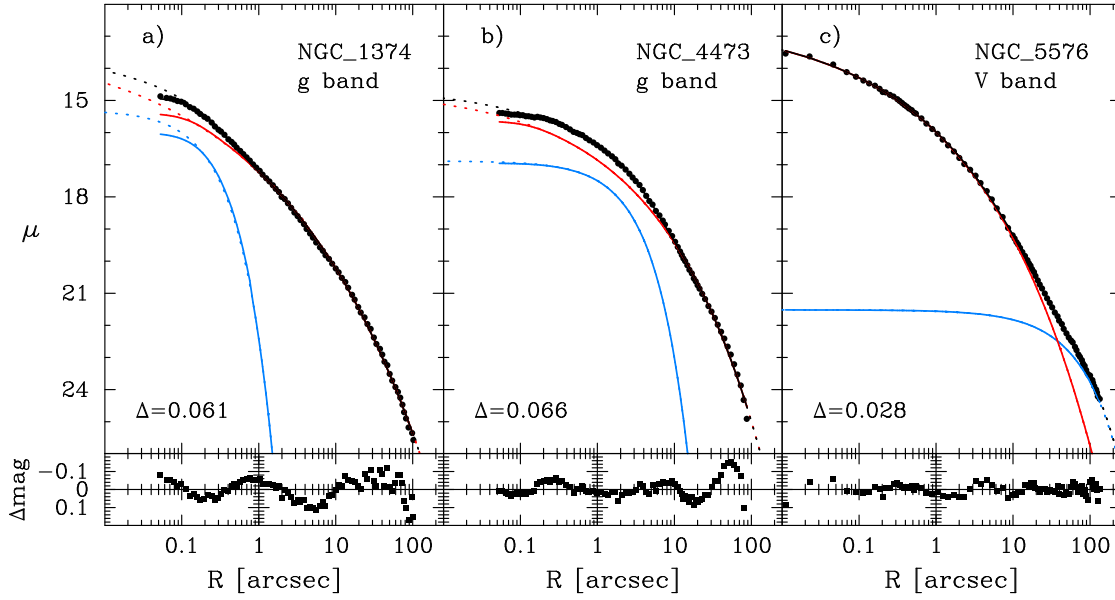


FIG. 7.— Double Sérsic model fits to the surface brightness profile of NGC 1374 (inner exponential + Sérsic), NGC 4473 (inner exponential + Sérsic) and NGC 5576 (inner Sérsic + outer Sérsic), see the text for details. The $\sim 100''$ geometric mean light profiles for NGC 1374 and NGC 4473 were taken from Turner et al. (2012) and Ferrarese et al. (2006), respectively. For NGC 5576, we use the Lauer (2012) composite (deconvolved *HST* data of Lauer et al. 2005 at $R \lesssim 10''$ + ground-based data at $R \gtrsim 10''$) major-axis light profile which extends out to $\sim 100''$. In contrast to Lauer (2012, his Fig. 1) and Lauer et al. (2005), our modelling (as in Dullo & Graham 2012) reveals the absence of depleted cores in these galaxies. The rms residuals, Δ , are shown in each panel.

9.1.6. NGC 6849

NGC 6849 is classified as an isolated, barred lenticular (SB0) galaxy in the RC3. It is also classified as an elliptical galaxy in the ground-based studies of Saraiva et al. (1999) and de Souza, Gadotti & dos Anjos (2004). In contrast to the findings of Saraiva et al. (1999), the F555W/*HST* unsharp-masking (Appendix B, Fig. 8) appears to suggest the presence of a bar in this galaxy. Fig. 2 illustrates that the ellipticity of this galaxy increases towards larger radii, which makes it the flattest in our sample. As shown in Fig. 3, the 3-component bulge-bar-disk luminosity profile is well fit by the the core-Sérsic bulge plus Ferrers bar plus exponential disk decomposition model with an rms residual of $\sim 0.04 \text{ mag arcsec}^{-2}$.

9.2. Comments on Dullo & Graham (2012)

Commenting on Dullo & Graham (2012), Lauer (2012) presented Sérsic model fits to the outer regions of composite light profiles (using the inner $10''$ *HST* profiles from Lauer et al. 2005 combined with ground-based profiles out to $\sim 100''$ taken from the literature) for three galaxies which Dullo & Graham (2012), and others, had shown not to possess depleted cores: NGC 1374, NGC 4473 and NGC 5576. Lauer’s (2012) fits suggested the presence of depleted cores relative to his outer Sérsic model. He therefore claimed that Dullo & Graham (2012) had misclassified these three galaxies as coreless Sérsic galaxies due to an incorrect application of the Sérsic model to radially limited $10''$ light profiles taken from Lauer et al. (2005). However, there were already $\sim 100''$ high-resolution *HST* profiles published for these galaxies that had been well fit using Sérsic models with no central light deficit (Turner et al. 2012, NGC 1374; Ferrarese et al. 2006 and Kormendy et al. 2009, NGC 4473; Trujillo et al. 2004, NGC 5576). Fig. 7 shows that the light profiles for these galaxies, covering a large radial extent, are described by the sum of two Sérsic profiles without any partially depleted core. The reason for these two-component models is detailed below. Basically, taking into account additional information, such as the presence of tidal material and/or kinematic substructure can help to identify the required components of a fit. In general, we recommend showing the residuals about one’s fitted model, as they can reveal if the large-scale curvature in the radial light distribution is well matched, and we advise against subjectively restricting the fitted radial range.

9.2.1. NGC 1374

Turner et al. (2012) fit a PSF-convolved Sérsic model to this galaxy, with no evidence for a depleted core. In Dullo & Graham (2012) we revealed that there is actually an additional component at the center of this galaxy. In Fig. 7a, we show our (PSF convolved) nuclear disk + Sérsic model fit to the light profile of NGC 1374 taken from Turner et al. (2012), see also the fit presented in Dullo & Graham (2012) to the inner $\sim 10''$. Some small (in amplitude), large-scale residual is present in Fig. 7a. The rotation curve in Graham et al. (1998, see also Longo et al. 1994) revealed that this galaxy rotates out to $40''$, suggesting the presence of an additional component which may be the cause of some of the residual structure about our exponential (for the nuclear disk) plus $n = 4.3$ Sérsic (for the underlying host galaxy light) model.

9.2.2. *NGC 4473*

Ferrarese et al. (2006) fit a PSF-convolved Sérsic model to NGC 4473, with no depleted core. Kormendy et al. (2009) identified a central light excess in this galaxy, above their adopted Sérsic ($n \approx 4$) fit, and they remarked that the extra light is due to a known counter-rotating embedded stellar disk (Emsellem et al. 2004; Cappellari & McDermid 2005; Cappellari et al. 2007). Fig. 7b shows our convolved exponential disk + Sérsic bulge model for this galaxy’s light profile taken from Ferrarese et al. (2006). We fit an exponential $n = 1$ function to the counter rotating disk, and find that a Sérsic $n \sim 3$ model fits the underlying galaxy light. Furthermore, Pinkney et al. (2003) remarked that this galaxy has unusual parameters from their Nuker model fit. They found that it has i) the smallest α value of their sample (i.e. a broad transition region between the inner and outer Nuker model power-law profiles) and ii) a very steep β value (the steepest from all the galaxies modelled by Byun et al. 1996). As warned in Graham et al. (2003), this is what one expects when fitting the Nuker model to what is actually a Sérsic profile with a low value of n and no depleted core. Pinkney et al. (2003) additionally remarked that the absolute magnitude of this galaxy is consistent with the “power-law” galaxies, i.e. those without depleted cores.

9.2.3. *NGC 5576*

Trujillo et al. (2004) modelled the deconvolved $100''$ light profile of NGC 5576 with the Sérsic model, finding no depleted core. Kim et al. (2012, their Fig. 5) showed that NGC 5576 and the barred S0 NGC 5574 are an interacting pair (see also Tal et al. 2009) having a long tidal tail, which extends out to 60 kpc in their $3.6 \mu\text{m}$ image. They showed the presence of tidal disturbances in the outskirts (from $1'$ to $2'$) of NGC 5576 because of this interaction. In Fig. 7c, we therefore fit a double Sérsic model to the light profile of NGC 5576 presented in Lauer (2012)⁶. We find that the central galaxy light distribution is well fit with an inner $n \sim 3.5$ Sérsic model, and the extra light, which is likely to be due to the re-distribution of material from the minor to the major-axis as a result of the tidal interaction, is described by an outer $n \sim 1.2$ Sérsic model. Kim et al. (2012) also fit a double Sérsic model (an inner $n = 3.45$ Sérsic model plus an outer $n = 1.48$ Sérsic model) to their light profile which is sampled from $R = 11''.8$ to $247''.5$. In general agreement with this and the inner $n \sim 4.5$ Sérsic model fit presented in Trujillo et al. (2004), our $n \sim 3.5$ Sérsic fit to this galaxy’s inner light distribution (Fig. 7c) not only shows the absence of a central luminosity deficit in this galaxy, but is also consistent with its magnitude $M_V = -21.11$ mag and velocity dispersion $\sigma = 171 \text{ km s}^{-1}$ (see Graham et al. 2001, their Fig. 13; Dullo & Graham 2012, their Fig. 14). This is in contrast to the single-component $n \sim 8$ Sérsic fit by Lauer (2012, their Fig 1).

We also note that, contrary to the claim by Lauer (2012), Dullo & Graham (2012, their section 4) explicitly noted that the spurious downward departure in the inner light profile of NGC 4486B (relative to the inward extrapolation of its outer Sérsic profile) is due to the presence of a double optical nucleus, rather than a typical depleted core. Coupled with NGC 4458, NGC 4478 and NGC 7213, we therefore have that seven of the 39 galaxies (i.e. $\sim 18\%$) classified as “core” galaxies according to the Nuker model analysis by Lauer et al. (2005), do not have central stellar deficits relative to their outer Sérsic profiles and are therefore not identified as “core-Sérsic” galaxies. Such ‘mismatches’ will be most prevalent among galaxy samples fainter than $M_B \approx -20.5$ mag that contain spheroids with low Sérsic indices and thus have relatively flat inner cores that are not depleted of stars.

The ATLAS 3D galaxy sample used by Lauer (2012) is dominated by early-type galaxies with magnitudes up to ~ 3 mag fainter than $M_B = -21$ mag — many of which are two-component lenticular galaxies (Emsellem et al. 2011). As such, application of the Nuker model may identify many ‘cores’ ($\gamma < 0.3$) among these galaxies which do not actually possess partially-depleted cores relative to their spheroid’s outer Sérsic profile. The Nuker model classification may therefore substantially blur the actual connection between the dry merger scenario, as described by Faber et al. (1997), and the existence of depleted cores from coalescing black holes. We thus advocate the core-Sérsic model and point readers to additional important reasons for this that are discussed in Graham et al. (2003) and Dullo & Graham (2012).

10. APPENDIX B

Fig. 8 shows distinct features in NGC 3607 (left), NGC 3706 (middle) and NGC 6849 (right).

⁶ Lauer (2012) noted that his ground-based profile for NGC 5576 was provided by Michard & Marchéal (1993), however this galaxy

was not actually included by those authors.

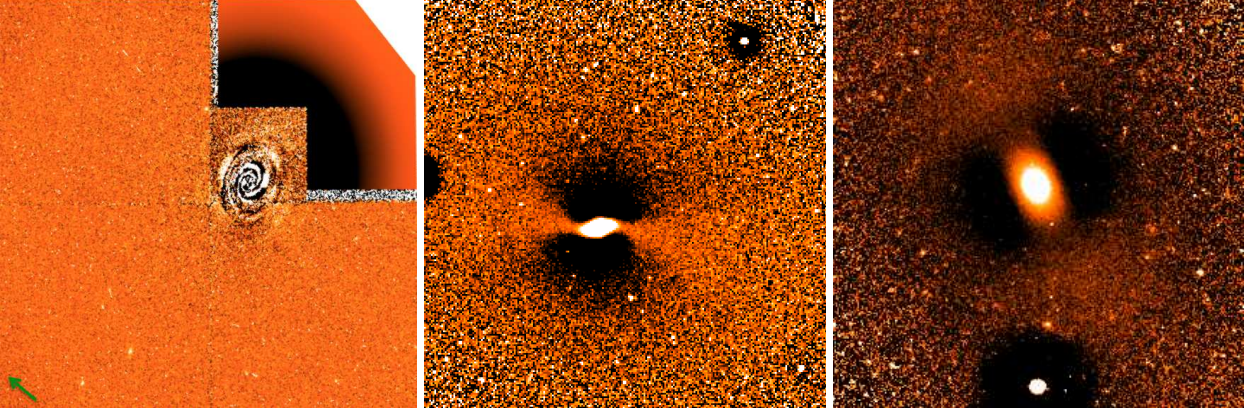


FIG. 8.— Left: Residual image of NGC 3607 obtained by subtracting our symmetrical image model from the original V -band image of the galaxy observed using the *HST*/WFPC2 camera. A dust disk is seen in the central region of the galaxy, see the Appendix A text for a further description. Middle: *HST* WFPC2/F555W PC $15'' \times 15''$ unsharp masked image of NGC 3706 showing an edge-on nuclear stellar ring (see Fig. 3 and Lauer et al. 2002, their Figure 1). Right: *HST* WFPC2/F555W PC $15'' \times 15''$ unsharp masked image of NGC 6849 showing an inner bar. For NGC 3607, north is in the direction of the arrow. North is up for NGC 3706 and NGC 6849.